Strands For Wood Composites: Mechanics & NIRS Based Nondestructive Testing

by

Neil Kohan

A thesis submitted to the Graduate Faculty of
Auburn University
in partial fulfillment of the
requirements for the degree of
Master of Science

Auburn University
December 12, 2011

Keywords: forest products, nondestructive testing, wood composites

Approved by

Brian Via, Chair, Assistant Professor of Forestry and Wildlife Sciences
Honorio Carino, Professor of Forestry and Wildlife Sciences
Steven Taylor, Professor of Biosystems Engineering

Abstract

Improvements in silvicultural techniques have allowed for rapid growth and shorter rotation age of southern pine species utilized for structural wood components. However, the rapid growth results in lumber consisting largely of juvenile wood. Juvenile wood is not desirable for solid lumber products as it possess lower strength qualities than mature wood. Therefore smaller diameter trees yielding lower quality wood have been effectively utilized in production of composite products such as oriented strand board (OSB) and oriented strand lumber (OSL). By using smaller diameter, short rotation plantation trees, composite products reduce the stress placed on mature stands and allow land owners to generate income from forests in shorter intervals. However, greater environmental and economical benefits could be realized through better utilization of OSB material streams. Better utilization will result in lower resin consumption, lower transportation cost, and reduced stress on existing forest stands. Currently OSB is produced with little regard for wood flake properties, with all flakes considered equivalent in mechanical properties. By effectively utilizing flakes throughout the OSB profile it will be possible to engineer high strength lightweight composites. It is the aim of this project to utilize NIR as a method to characterize flakes based on predicted mechanical properties (stiffness and strength).

NIR techniques are proven effective at rapidly predicting wood quality and strength. Industry has not yet embraced NIR spectroscopy as a method for nondestructive testing. However, applied research such as this project may generate interest in application of NIR techniques to wood composite manufacturing such as oriented strandboard or oriented strand lumber.

Table of Contents

List of Figures

List of Tables

List of Equations

Chapter 1 Introduction

Wood has long been the most widely used building material. Excellent strength, durability, and workability, coupled with widespread availability of woody resources have made wood products the ideal engineering material. While wood was initially chosen over other materials for the aforementioned properties, it is now the choice among building materials because of its renewable nature. Unlike other building materials, wood products are fully renewable. By examining embodied energy, that is all the energy required to produce and ship the material, wood is clearly the more environmentally-friendly of common building materials (concrete, steel, plastic) as it provides energy and emission reduction of other materials. The limited energy required to produce wood products, and the industry reliance on biomass derived energy (up to 60%) are both responsible for wood's low embodied energy (Murray et al. 2006). Furthermore, wood is an organic material, meaning carbon is a key component. Carbon's role in global climate change has come to the forefront of environmental concern in recent years. Although the exact mechanisms of climate change are not fully understood, the role of forests and wood products in the carbon cycle are well documented. Forests themselves store a considerable amount of carbon in living trees, forest debris, and soil. Eventually decay of wood in forests leads to release of carbon back into the atmosphere, but through use of wood products this carbon can stored in durable products (US FPL 2010). Carbon sequestered in wood products was estimated to be 680 million metric tons in 2001 (Skog 2008).

Although its natural origin makes wood the ideal building material, it is also to blame for the variation in wood quality. Wood exhibits variation in mechanical and physical properties

between and within species (US FPL 2010). Thus, widely available species exhibiting ideal mechanical and physical properties have been utilized for wood and composite products (US FPL 2010). The variation in wood quality is also influenced by silvicultural practices (Zobel 1992). Wood quality has been shown to be affected by pruning (Megraw 1985), fertilization (Posey 1965, Gladstone & Gray 1972), thinning (Baldwin et al. 2000), and stand density (Biblis et al. 1995, 1997). But perhaps of most influence on wood quality is the age at harvest (Martin 1984, Schultz 1999). The age at harvest is most influential as trees harvested on shorter rotations contain more juvenile wood. Juvenile wood is the first wood formed by a young tree, and is found closest to the pith. Juvenile wood cells do not fully mature in the young tree as their growth is still affected by the apical meristem (Panshin & De Zeeuw 1980). While the exact function of juvenile wood in the tree is not known, its effects on wood properties are well documented. Juvenile wood is characterized by shorter tracheids, higher microfibril angle (including S2 layer), a lower percentage of latewood, thinner cell walls, higher lignin content, and lower cellulose content. All of these factors lead to increased shrink-swell properties, and lower strength properties compared to mature wood (Larson et al. 2001, US FPL 2010). The transition from juvenile wood to mature wood is not abrupt, and varies from species to species, but research estimates consider wood from the 5^{th} to 20^{th} ring to contain juvenile wood (Bendtsen & Senft 1986). While it is known that extending rotation periods would both increase wood quality and produce environmental benefits (Lippke et al. 2004), most commercial plantation wood is characterized by a high percentage of juvenile wood as result of short rotations (Pearson & Gilmore 1971).

Composite panels derived from wood were developed in response to demand for building products, and to utilize smaller trees, like those grown in plantations. Of specific interest to this research project are oriented strandboard (OSB) panels. OSB panels are made from short wood strands that are cut from small diameter, average of 20.5cm, southern yellow pine and hardwood species (McKeever 2000). Strands are dried and blended with phenol-formaldehyde (PF), diphenylmethane diisocyanate (MDI), or other resins and wax. The strands are then oriented and formed into loose mats which are hot-pressed to cure the resins and consolidate strands into panels. OSB was introduced to compete with plywood, which is unable to utilize the small diameter trees utilized in OSB plants. The lower cost of manufacturing and similar qualities have led to OSB overtaking a large portion of plywood market share, with the exception of some higher value-added sectors still relying on plywood (Maloney 1996, Spelter 2006).

Increasing uniformity in production is of paramount importance to OSB manufacturers. By improving uniformity, plants are able to more efficiently utilize the wood resource. While improving uniformity may not increase the mean mechanical properties of OSB, it will allow better control of the lower 5^{th} percentile properties (Lam 2001). In an industrial operation, panels are produced to exceed a lower threshold of mechanical properties, as required by both load and resistance factor design (LRFD) and allowable stress design (ASD) formats (AWC 2006). Reducing variation and producing a uniform OSB panel is dependent on numerous production factors such as strand in-plane orientation, resin content, strand length, strand thickness, and fines content (Barnes 2000). In addition, the quality of the composite panel is dependent upon the quality of the raw material used (Deomano & Zink-Sharp 2004). Thus OSB panel mechanical properties are a function of mechanical properties of strands as well as production factors (Xu & Suchsland 1998). Because of this, OSB panels are affected by the

presence of juvenile wood strands. Pugel et al. (1990a) investigated the affect of juvenile wood on mechanical properties of numerous composites. When used to produce flakeboard, a precursor to OSB, researchers were able to produce pure juvenile wood panels with mechanical properties similar to mature wood panels. However, to reach the same mechanical properties, a panel density with a higher compaction ratio was utilized for juvenile wood panels. The increased compaction ratio means the juvenile wood panels require 20% more wood compared to mature wood panels (Pugel et al. 1990a). Because of the higher compaction ratio, juvenile wood flakeboards exhibited greater thickness swell and lower durability (in terms of residual strength after ovendry-vacuum-pressure-soak) compared to mature wood panels. Increasing the compaction ratio to improve mechanical properties of juvenile wood panels is common practice at southern OSB mills, which results in higher wood use and reduced dimensional stability (Pugel et al. 1990b). The problems associated with flakeboard panels produced from juvenile wood would also arise in OSB production. However, it has been shown that properties will not suffer if panel furnish is less than 70% juvenile wood (Cloutier et al. 2006). Therefore implementation of an online nondestructive testing method could alert manufacturers of changes in wood strand quality, in this case strand strength, which varies between mature wood and juvenile wood.

A rapid nondestructive testing method that has been successful in predicting wood quality and online grading of sawn lumber is near infrared spectroscopy (Fujimoto et al. 2010). When applied to composite production, NIRS techniques were able to incorporate wood quality information into a process modeling system (Sjöblom et al. 2004). The results showed the potential of NIRS to monitor wood quality, allowing proactive changes to composite process parameters. By reducing variation in the final product, costs could be reduced by 2.8 euros/m^3

produced (Sjöblom et al.2004). If a similar system is applied to OSB production, similar cost savings may be possible.

To date significant research has been conducted regarding NIRS as a tool for nondestructive evaluation of solid wood. However, limited research on NIRS and thin wood strands exist, and no research on NIRS as a tool for evaluating mechanical properties of strands has been published. Therefore this study was conducted to meet the following objectives:

1. Develop a methodology for determining mechanical properties of wood strands like those utilized in commercial OSB production
2. Evaluate the efficacy of NIRS to predict mechanical properties of OSB strands

1.1 References

American Wood Council (AWC). (2006). *Wood Design Package: Manual for engineered wood construction* (Vol. 3). American Forest & Paper Association.

Baldwin, V. C., Peterson, K. D., Clark, A., Ferguson, R. B., Strub, M. R., & Bower, D. R. (2000). The effects of spacing and thinning on stand and tree characteristics of 38-year-old loblolly pine. *Forest Ecology and Management*, *137*(1-3), 91–102.

Barnes, D. (2000). An integrated model of the effect of processing parameters on the strength properties of oriented strand wood products. *Forest products journal*, *50*(11/12), 33–42.

Bendtsen, B. A., & Senft, J. (1986). Mechanical and anatomical properties in individual growth rings of plantation-grown eastern cottonwood and loblolly pine. *Wood and Fiber Science*, *18*(1), 23–38.

Biblis, E. J., Carino, H., Brinker, R., & McKee, C. W. (1995). Effect of stand density on flexural properties of lumber from two 35-year-old loblolly pine plantations. *Wood and fiber science*, *27*(1), 25–33.

Biblis, E. J., Carino, H. F., & Brinker, R. (1997). Flexural properties of lumber from two 40-year-old loblolly pine plantations with different stand densities. *Wood and fiber science*, *29*(4), 375–380.

Cloutier, A., Ananias, R. A., Ballerini, A., & Pecho, R. (2006). Effect of radiata pine juvenile wood on the physical and mechanical properties of oriented strandboard. *Holz als Roh- und Werkstoff*, *65*(2), 157-162.

Deomano, E., & Zink-Sharp, A. (2004). Bending Properties of Wood Flakes of Three Southern Species. *Wood and Fiber Science*, *36*(4), 493-499.

Fujimoto, T., Kurata, Y., Matsumoto, K., & Tsuchikawa, S. (2010). Feasibility of Near-Infrared Spectroscopy for On-Line Grading of Sawn Lumber. *Applied spectroscopy*, *64*(1), 92–99.

Gladstone, W. T., & Gray, R. L. (1973). Effects of forest fertilization on wood quality. *Forest Fertilization. USDA Forest Service Gen. Tech. Rept. NE-3*.

Lam, F. (2001). Modern structural wood products. *Progress in Structural Engineering and Materials*, *3*(3), 238–245.

Larson, S. P., & others. (2001). Formation and properties of juvenile wood in southern pines.

Lippke, B., Perez-Garcia, J., & Comnick, J. (2004). Corrim Fact Sheet 3. Consortium for Research on Renewable Industrial Materials

Martin, J. W. (1984). Forest management practices that will influence product characteristics of the changing wood resource. *Proc. Symposium on Utilization of the Changing Wood Resource in the Southern United States. North Carolina State University, Raleigh, NC* (pp. 115–123).

Maloney, T. M. (1996). The family of wood composite materials. *Forest Products Journal*, *46*(2), 19–26.

McKeever, D. B. (2000). Demand for Engineered Wood Products. *Techlines.*

Megraw, R. A., & Megraw, R. A. (1985). *Wood quality factors in loblolly pine*. Tappi.

Murray, B., Nicholson, R., Ross, M., Holloway, T., & Patil, S. (2006). Biomass energy consumption in the forest products industry. *US Dept. of Energy, RTI International*.

Panshin, A. J., & De Zeeuw, C. (1980). *Textbook of wood technology.* McGraw-Hill Book Co.

Pearson, R. G., & Gilmore, R. C. (1971). Characterization of the strength of juvenile wood of loblolly pine. *Forest Products Journal*, *21*(1), 23–30.

Posey, C. E. (1965). The effect of fertilization upon wood properties of loblolly pine. *Proceedings of the 8th Southern Conference on Forest Tree Improvement, Savannah. June 16–17, 1965, Savannah GA* (pp. 126–130).

Pugel, A. D., Price, E. W., & Hse, C. Y. (1990a). Composites from southern pine juvenile wood. Part 1. Panel fabrication and initial properties. *Forest products journal*, *40*(1), 29–33.

Pugel, A. D., Price, E. W., & Hse, C. Y. (1990b). Composites from southern pine juvenile wood. Part 2. Durability and dimensional stability. *Forest products journal*, *40*(3), 57–61.

Schultz, R. P. (1999). Loblolly–the pine for the twenty-first century. *New forests*, *17*(1), 71–88.

Sjöblom, E., Johnsson, B., & Sundström, H. (2004). Optimization of particleboard production using NIR spectroscopy and multivariate techniques. *Forest products journal*, *54*(6), 71–75.

Skog, K. E. (2008). Sequestration of carbon in harvested wood products for the United States. *Forest Products Journal and Index*, *58*(6), 56–72.

Spelter, H., McKeever, D. B., Alderman, M., & (US), F. P. L. (2006). *Status and trends: profile of structural panels in the United States and Canada* (Vol. 636). US Dept. of Agriculture, Forest Service, Forest Products Laboratory.

US FPL (2010). Wood Handbook: Wood As An Engineering Material.

Xu, W., & Suchsland, O. (1998). Modulus of elasticity of wood composite panels with a uniform vertical density profile: A model. *Wood and fiber science*, *30*(3), 293–300.

Zobel, B. (1992). Silvicultural effects on wood properties. *IPEF International*, *2*, 31–38.

Chapter 2 Literature Review

2.1 Wood Structure

2.1.1 on the Hierarchical structure of wood

Wood is unique among engineering materials in that it is an organic renewable resource exhibiting orthotropic mechanical and physical properties. Wood is the xylem, or fluid conducting tissue, of two groups of plants: *Angiosperms* and *Gymnosperms*, commonly known as hardwoods and softwoods respectively. The xylem is produced by the cambium. Because of its organic nature, genetic and environmental factors are a source of variation in material properties. To understand the complex structure of wood it is best to separate the wood structure into three hierarchial groups: the nano, micro, and meso scales.

2.1.2 on the Nano-scale properties of wood

The nano-scale of wood 1 to 100 nm involves the chemical constituents of wood, their composition and arrangement. The three main chemical constituents of wood are cellulose, hemicelluloses, and lignin. Together these chemicals are arranged to form the basic units of the cell wall.

Cellulose is a long-chain polymer of β-D-glucopyranose units with a degree of polymerization exceeding 10,000. Monomer subunits allow for three hydrogen bonds, one of which bonds monomers together in cellulose chain through 1→4 glycosidic bonds. Throughout its length cellulose is crystalline in nature with intermittent amorphous, semi-amorphous, or accessible regions. The crystallinity of cellulose makes it extremely stiff as well as hydrophobic.

The average concentration of cellulose in wood is roughly 45 and 40 percent in angiosperms and gymnosperms respectively.

Hemicelluloses, not half-cellulose as the name suggests, are polymers composed of many different five and six carbon sugars. Unlike cellulose, hemicelluloses are highly hydrophilic due to amorphous nature and accessible hydroxyl groups. Side groups on hemicellulose prevent formation of crystalline regions so they exist in an amorphous state with a degree of polymerization between 500 and 1,000. Concentrations and structures of hemicellulose vary between angiosperms and gymnosperms, but compose approximately 20 to 30 percent of the cell wall.

Lignin is a disordered phenolic polymer with 3D structure. Lignin is highly hydrophobic and accounts for roughly 30 percent of the cell wall and nearly 100 percent of the middle lamella.

Within the cell wall the three chemical constituents are arranged differently. Cellulose chains exist in tight bundles, with hydrogen bonds forming between adjacent glucose molecules. A bundle of 50 to 80 cellulose molecules is referred to as an elementary fibril, roughly 3.5 by 3.5nm in cross section. Elementary fibrils are further arranged into microfibrils with 3.5 by 10nm cross section. The cellulose microfibrils provide stiffness of wood in longitudinal and transverse directions, as cellulose has a much higher elastic modulus compared to hemicelluloses or lignin. Cellulose microfibrils will not associate with lignin, but will bind with hemicelluloses (Kollmann 1968, Panshin 1970, US FPL 1974, Winandy 1985, Haygreen 1996, Cramer 2005).

Hemicelluloses associate with both lignin and cellulose in the cell wall. The hemicelluloses act as a matrix for the cellulose microfibrils. Together the cellulose microfibril in hemicellulose matrix is referred to as holocellulose. The lignin acts as an encrusting agent for

the holocellulose fraction of wood. In theory the hemicellulose matrix acts as an adhesive between the cellulose microfibrils and surrounding lignin. Acting as adhesive, hemicelluloses do not impart much tensile strength to wood material, but lignin provides strength in both compression and shear. The longitudinal modulus is the highest in all three chemicals, followed by transverse modulus, and finally shear modulus (Kollmann 1968, Panshin 1970, US FPL 1974, Haygreen 1996).

Under stress, wood at the nano-level behaves like a reinforced concrete block wall. Cellulose can be likened to steel rebar, providing tension strength parallel to its length. The hemicellulose matrix acts as the concrete fill, resisting shear and compressive forces. The lignin, represented by the concrete masonry units, also resists shear and compressive forces, but without concrete fill (hemicelluloses) it would have no association with steel rebar (cellulose).

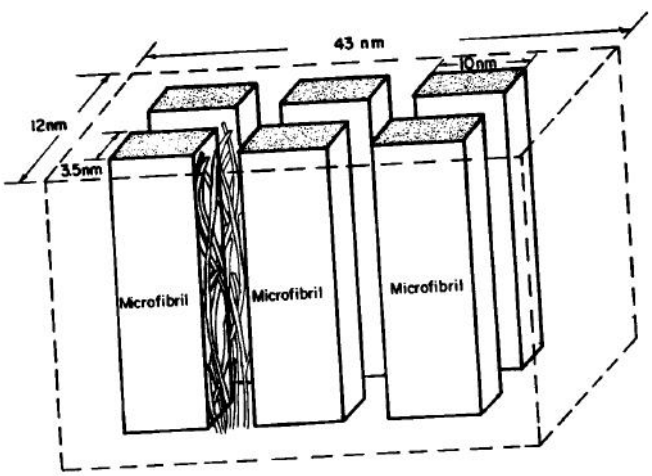

Figure 2.1 Arrangement of microfibrils in the cell wall (Bodig & Jayne 1982)

2.1.3 on the Micro-scale properties of wood

Holocellulose and lignin materials are further organized into laminae, which are then combined to form cell wall layers: middle lamella, primary layer, and three secondary layers (S_1,S_2, S_3). In each of the layers cellulose microfibrils are aligned in helical pattern at an angle to the long axis, referred to as the microfibril angle (MFA). The MFA has a considerable impact on wood stiffness, with higher angles resulting in lower longitudinal elastic modulus. The middle lamella is a region composed mainly of lignin which serves as a bond between cells. The primary cell wall does not provide structural strength as cellulose microfibrils are randomly oriented throughout the thin layer. The primary cell wall layer is often grouped together with the middle lamella in a structure referred to as the compound middle lamella (CML), which is 0.6 to 1.5 μm in thickness. The secondary cell wall forms through thickening of cell wall after primary wall is formed. The secondary cell wall is considerably thicker than the compound middle lamella, often more than 10μm thick. The secondary wall is further split into three layers, S1, S2, and S3 in which microfibrils exhibit ordered parallel arrangement. The S1 layer is 0.1 to 0.35 μm thick, the thinnest of the 3 sublayers, with a MFA of 60 to 80 degrees. The S2 layer is the thickest of the sublayers, between 1 and 10 μm, and accounts for roughly 80% of the cell wall thickness. The MFA in the S2 layer is the lowest of the sublayers, between 5 and 30 degrees in normal wood (Plomion 2001). Because the S2 layer accounts for much of the cell wall, it is exceptionally important for overall wood strength, and its MFA is of particular importance to elastic modulus (Harris and Meylan 1965). The S3 layer has MFA in range of 60 to 90 degrees, and is much thinner than the S2 and usually between 0.5 and 1.10 μm thick. (Plomion 2001).

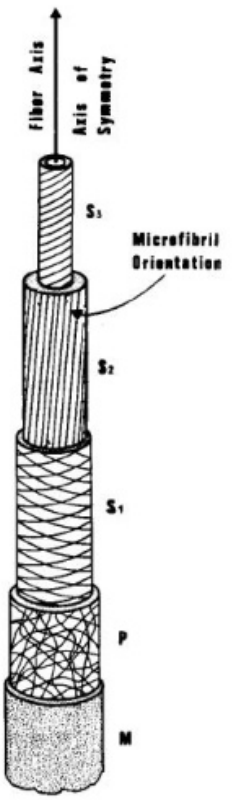

Figure 2.2 Cell wall model of softwood tracheid (Bodig & Jayne 1982)

On the microscopic level, cell wall layers are organized into a variety of tubular cells. The variation of cell size, shape, and type in Angiosperms is quite large, but Gymnosperms possess mainly one cell type (and only one type of structural importance): the tracheid. The tracheid in Gymnosperms serves dual functions: conduction of liquids through the tree, and mechanical strength. Wood cells are layered to form growth rings, also called annual increments. Within the growth ring, wood varies in density from start to finish. In Southern yellow pine (SYP), wood produced early in the growing season, called earlywood or springwood, is of lower density (~0.28 g/cm^3) with larger lumen diameter and thinner cell wall. Higher density wood (~0.60 g/cm^3) produced later in the growing season is latewood or

summerwood. Latewood has a thicker cell wall with smaller lumen diameter. Gymnosperms also have ray cells, which are oriented perpendicular to the tangential plane and serve as fluid conducting and storage cells. Density and MFA differences between earlywood and latewood have a great impact on elastic properties, thus latewood in SYP is more than 50 percent stronger and stiffer than earlywood with average E_L of 4.34 GPa in earlywood and 9.88 GPa in latewood (GL_T of 0.77 GPa in earlywood and 1.59 GPa in latewood) (Biblis 1969, Cramer 2005). As a result the latewood region has the most influence on mechanical properties (Mork 1928, Kollmann 1968, Panshin 1970, US FPL 1974, Winandy 1985, Haygreen 1996, Cramer 2005).

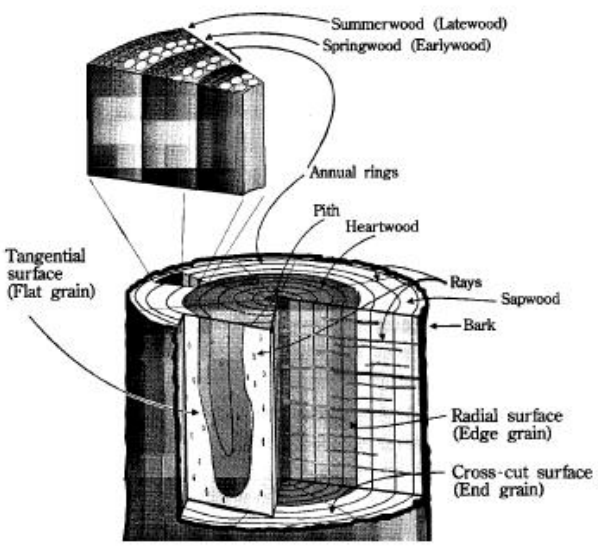

Figure 2.3 Macroscopic features of wood (Marra 1992)

2.1.4 on the Macro-scale properties of wood

Wood is an anisotropic material. The term anisotropic means that wood exhibits different mechanical properties along the three major axes. Axes in wood are defined by growth ring pattern, radial, tangential, and longitudinal. The radial axis extends from the pith of the tree

outward to the edge. The tangential axis is the tangent along the growth rings. The longitudinal axis runs parallel the length of the tree. Given the alignment of fibers along an axis wood is strongest in the longitudinal direction. Strength in compression, tension, and also stiffness is highest parallel to the grain (Panshin 1970).

Wood exhibits great variability between and within species. Within species variability is result of both genetics and silvicultural factors. Silvicultural factors often have the greatest impact on wood quality. In the Southeastern United States, silvicultural techniques call for short rotations on Southern pine plantations. Conditions in plantations directly impact wood quality and the short rotations, typically 12 to 18 years, produce lumber with high prevalence of juvenile wood characteristics (Benson 1930, Bendtsen 1978, Biblis 1995).

2.2 on the properties of Juvenile Wood

For the first five to twenty years of growth, wood produced in the Southern pine cambium is heavily influenced by apical meristem growth in the crown. As it is produced during the early stages of tree growth this wood is referred to as juvenile wood, in contrast to mature wood produced after the first twenty years. Juvenile wood differs from mature wood anatomically, chemically, and physically. Although chemical differences are present it is safe to focus purely on physical differences between juvenile and mature wood for mechanical considerations.

Certain properties decrease from juvenile wood to mature wood. First, juvenile wood typically has a higher microfibril angle compared to mature wood. A higher microfibril angle results in a lower longitudinal elastic modulus and undesirable physical properties like increased longitudinal shrinkage. Spiral grain is also more prevalent in juvenile wood, with decreasing occurrence as the tree matures. Spiral grain is the condition in which fiber grain, not to be

confused with visible grain, is not approximately parallel to longitudinal axis of wood. Residual moisture content is generally higher in juvenile wood, decreasing with transition into mature wood. This is a result of chemical and physical differences between juvenile wood and mature wood. Mature wood has a higher lignin, extractives, and cellulose content than juvenile wood. Juvenile wood also has more hemicelluloses than mature wood (Uprichard 1971, Harwood 1971).

Other properties increase as a tree ages and produces mature wood in place of juvenile wood. Specific gravity, the ratio of wood density to the density of water at 4°C, is low in juvenile wood increasing in the mature wood. Cell wall thickness and cell length also increase from juvenile wood to mature wood. Juvenile wood is also characterized by a lower percentage of latewood, or summerwood, compared to mature wood (Kollman 1968, Panshin 1970, USFPL 1974, Bendtsen 1978).

These properties of juvenile wood are all undesirable, and as a result juvenile wood is of much lower quality than mature wood. Modulus of rupture, tensile strength, and bending elastic modulus are all lower in mature wood than juvenile wood (Bendtsen 1978, Panshin 1970, Smith 1986, Biblis 1993, Briggs 1994). In turn, composites made from juvenile wood are also weaker than composites made from mature wood when produced with the same volume of wood. Juvenile wood composites are weaker in bending, shear, and compression, and also exhibit greater shrinkage and swell (Jo 1981, Geimer 1980, 1986, 1997). Juvenile wood also exhibits a nonlinear stress-strain relationship below the proportional limit, unlike the linear behavior of mature wood (Rowland 2004).

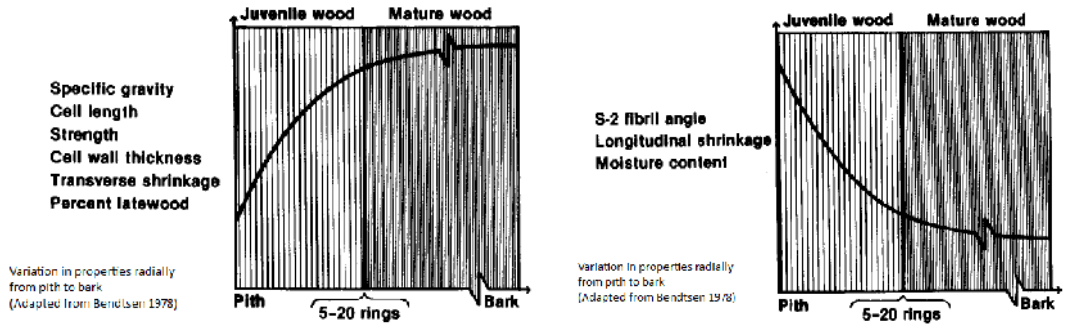

Figure 2.4 Wood quality in juvenile & mature wood (Bendtsen 1978)

2.3 On the factors affecting wood strength

The natural variability of wood creates unique problems for wood as an engineering material. Many of the variable factors have direct impact on wood strength. Specific gravity, being an index of wood substance in a specific volume, is an excellent indicator of mechanical properties in wood. Crushing strength parallel to grain, fiber stress at elastic limit in bending, and shear strength along the grain vary in direct proportion with specific gravity (Record 1914, Wangaard 1950, Bodig 1982). The relationship is in fact linear, with original strength (S) and specific gravity (g) varying directly with reduced strength (S') and specific gravity (g') for any given mechanical property (n) (US Dept Defense 1951):

Equation 2.1 Specific gravity & strength (US Dept Defense 1951)

$$\frac{S}{S'} = \left(\frac{g}{g'}\right)^n$$

Grain defects such as spiral grain also greatly reduce mechanical strength of wood. Changes in grain angle reduce ability for stresses to transfer along long axis, resulting in lower strength properties (Record 1914, Wangaard 1950, US FPL 1974, Bodig 1982).

Although it can be controlled to some degree, moisture content is another factor limiting the strength of wood. Water can be found in wood as free water in cell cavities, or as bound

water within cell walls. Bound water limits strength by creating mechanical voids between wood microfibrils. These voids limit the ability of stresses to transfer between microfibrils. Without removing bound water shear strength, modulus of elasticity, and tensile strength of wood is moderately impacted. A high moisture content has a tremendous impact on modulus of rupture, and stress at elastic limit in bending (Record 1914, Wangaard 1950, US FPL 1974, Bodig 1982).

Mechanical strength of wood is also affected by changes in wood fiber length. Shorter fibers experience greater shear stress concentrations, and therefore reduced overall strength (Wellwood 1962). Higher microfibril angles also result in lower strength qualities (Kollmann 1968, Panshin 1970, US FPL 1974, Winandy 1985, Haygreen 1996, Cramer 2005). Strength reduction as result of changes in MFA can be accounted for using the Hankinson formula (Hankison 1921, Bodig 1982):

Equation 2.2 The Hankison Formula (Wellwood 1962)

$$N = \frac{PQ}{Psin^n\theta + Qcos^n\theta}$$

$N = strength\ at\ angle\ \theta$

$Q = strength\ \perp\ to\ grain$

$P = strength\ \parallel\ to\ grain$

$n = constant\ corresponding\ to\ mechanical\ property$

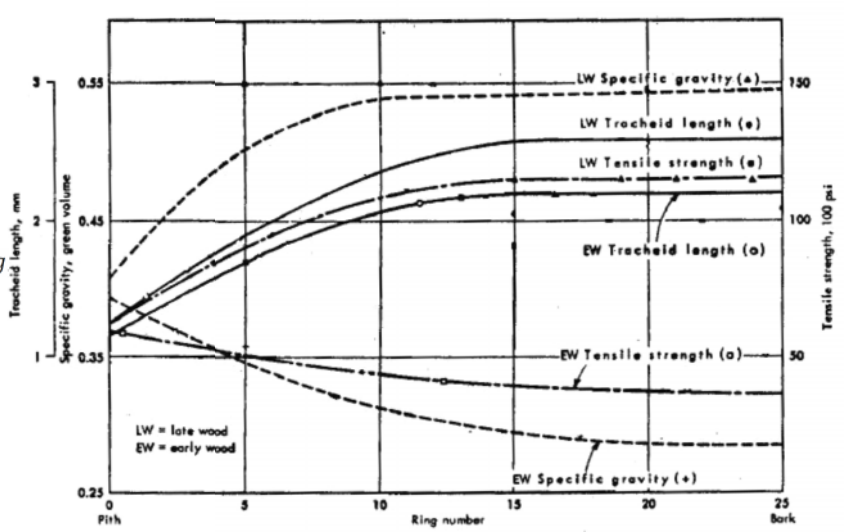

2.4 On the use of NIR spectroscopy to evaluate materials

Near infrared spectroscopy is an effective tool for nondestructive evaluation of materials from the nano to macro scale. NIR spectroscopy is based on absorption of light through the infrared region extending from 750nm to 2500nm. Absorption (A) of infrared light excites

molecules causing vibrations. Reflectance (R), light not causing vibrations, can be collected and measured with spectrophotometer. Absorption is then calculated by: $A = \log \frac{1}{R}$

With respect to wood material, NIR absorbance spectra show vibrations in bond structural groups: O-H, C-H, N-H. The absorbance spectra are generally quite complex due to vibration overtones, thus interpretation requires use of statistical models including partial least squares (PLS), multiple linear regression (MLR), and principal components regression (PCR) to draw correlations between spectra and measured characteristics. NIR has been effective at identifying characteristics relating to wood strength.

For the pulp and paper industry, NIR has been used to estimate chemical composition of wood. NIR has been proven effective at estimating lignin, cellulose, and hemicellulose concentration in wood. As early as 1997, NIR spectroscopy was used to evaluate the concentration of primary wood polymers and Kraft pulp yields of plantation hardwoods (Schimleck 1997). NIR spectroscopy has also been used to predict chemical content of Southern yellow pine wood from a wide-range of sites and growing conditions (Jones 2006).

Moisture content not only impacts strength of wood, but also affects processing. Production of composites such as OSB is sensitive to moisture content. Calibration equations for detecting moisture content of solid wood using NIR spectroscopy have been available for over a decade (Tsuchikawa 1996, Via 2005).

NIR is also an effective tool for rapidly evaluating the density of wood (Hoffmeyer 1995). Increases in wood density increase NIR absorbance. Via (2003) attributed partial sensitivity of NIR to density to increased absorbance at higher densities. Via went on to demonstrate a deviation from Beer-Lambert law at high densities of wood, similar to observations made on other materials. As stated, density and specific gravity are often used as

general indicators of wood strength. Grain angle has also been predicted through NIR spectroscopy. Estimation of grain angle using NIR is effective up to grain angles of 40°. Since a majority of strength loss is within the first 20°, accuracy to 40° is more than sufficient for estimation of strength properties (Tsuchikawa 1997, Grindl 2002, US FPL 1974, Marra 1992, Bodig 1982). NIR spectroscopy is also an effective method for estimation of microfibril angle. Along with microfibril angle, NIR spectroscopy can estimate fiber length (Schimleck 2004, Schimleck 2002, Marklund 1999). Based on characteristics predicted using NIR, it has been demonstrated as effective method for classifying juvenile and mature wood (Via 2003, Lestander 2008).

NIR has been proven effective at identifying or estimating characteristics correlated to wood strength. Research has also advanced to the point of using NIR to predict wood strength directly. Modulus of elasticity (MOE) and modulus of rupture (MOR) have been accurately predicted using NIR and various statistical techniques (Table 2.1). In addition, NIR can provide accurate prediction of maximum load for both compression and tension faces of beams (Andre 2006). Strength in bending, compression strength, and ultimate tensile strength are all readily predicted from NIR spectra (Lestander 2008, Tsuchikawa 2005).

NIR has not yet been utilized by industry despite current research showing value as nondestructive indicator of wood strength. Initial cost of NIR spectrophotometers may be partially to blame. However, reduced spectral range NIR spectrophotometers, which are more economical, have also been able to accurately predict MOE and MOR. Reduced ranges from 400nm to 1100nm produced solid results (Kelley 2004). Further research involving NIR and moving samples have produced good results and the concept is promising for adaptation of spectral techniques to the production environment (Thumm 2001).

Table 2.1 Selected NIRS literature in forest products industry

Properties	R-Square	Model type	Stress	Reference
MOE, MOR	0.29	PLS, PCR	Bending	Hoffmeyer & Pederson 1995
MOE, MOR	0.80-0.88	PLS	Bending	Schimleck 2001
MOE	0.55-0.72	PLS	Bending	Thumm & Meder 2001
MOE, MOR	0.89	PLS	Bending	Gindl 2001
MOE, MOR	0.85	PLS	Bending	Kelley 2004
MOE, UTS	0.53-0.74	PLS	Tension	Tsuchikawa 2005
MOE, MOR	0.73-0.89	PLS	Bending	Fujimoto 2008
MOE, MOR	0.83-0.87	MLR, PCR	Bending	Via 2009

Hoffmeyer and Pederson were the first to research NIRS as tool to predict mechanical properties of wood material, publishing their work in 1995. Hoffmeyer and Pederson conducted experiments on Norway spruce (*Picea abies*) samples with natural defects such as knots and slope of grain.

Some years later in 2001 Thumm and Meder conducted flexural tests on clear *Pinus radiata* after scanning samples over 400 to 2500 nm range. Static and dynamic scanning methods were utilized. Thumm and Meder also explored use of spectra pretreatment, using 1st and 2nd derivatives and achieved prediction coefficient of determinations of 0.55 to 0.72 for stiffness in bending.

In 2001, Schimleck utilized NIRS to predict MOR, MOE, and MFA of *Eucalyptus delegatensis* samples. Schimleck also used the 1st and 2nd derivatives to help develop PLS models that provided prediction R^2 over 0.80 for both MOR and MOE.

Again in 2001, Gindl investigated NIRS and MOR, MOE, and compressive strength of *Larix decidua*. Gindl included an investigation of NIR of compression wood as well as normal

wood. Gindl's results were similar to other literature with R^2 of 0.89 for prediction of elastic modulus in bending.

In 2004, Kelley investigated NIRS and flexural properties of *Pinus taeda*. In addition, Kelley looked at chemical properties and microfibril angle. Scans were made over 500 to 2500 nm range as well as a reduced spectral range of 650 to 1150 nm. NIRS was able to predict MOE in bending with R^2 of 0.85.

Tsuchikawa, in 2005, was the first to investigate NIRS and tensile properties. Tsuchikawa used clear Japanese red pine (*Pinus densiflora*) and Japanese zelkova (*Zelkova serrata*) for tensile testing. Tsuchikawa used statistical techniques for both prediction and interpretation. Tsuchikawa was able to assign specific wavelengths to strength parameters.

2.5 OSB Manufacturing

Oriented strand board (OSB) is an engineered composite of wood strands bonded with resin under heat and pressure. OSB panels are able to utilize smaller trees lacking straight bole, trees that are otherwise unfit for plywood production. The goal of wood composites is to engineer a panel or member that effectively distributes natural defects throughout its volume. By distributing natural defects throughout the product variability from element to element can be reduced, allowing for higher design values.

Production of OSB is a multi step process. Initially, strands are produced by flaking debarked log into thin strips. Generally these strips do not exceed 15 cm in length, 2.5 cm in width, or 1mm in thickness. Strands are cut radially or tangentially from the log. Strands are then dried in tumbling cylinders at high heat, due to the high surface area to volume ratio strands dry rather quickly. Strands are then blended, in tumbling blender, with resins. Strands are then

aligned, through mechanical means, into loose mats. The loose stand mats are pressed under heat and pressure to a certain thickness to achieve a certain density (US FPL 1974, Marra 1992). Strands in the surface layers are oriented parallel to the long axis of the panel. Since orientation is achieved through mechanical or electrostatic means, it is not absolute. However, strands are on average parallel to long surface though many strands may deviate to some degree. Surface layer strands are usually oriented perpendicular to the long axis. Cross-aligning the core strands increases dimensional stability of OSB panel. Cross-alignment also provides resistance to stresses occurring across panel width. OSB panels are typically designed to target density, as the relationship between density and strength has to this point, been the easiest factor to control in industry.

Resins are the adhesive used to bond wood strands together in a wood composite such as OSB. The most common adhesives used for OSB bonding are phenol-formaldehyde adhesives. There are many different phenolic resins but all fall into two distinct categories: resoles and novolac. Resins containing a higher molar concentration of formaldehyde compared to phenol are referred to as resoles. Resoles form cross-linked bonds, and do so under heat without addition of hardening agents. Resins containing more phenol than formaldehyde are known as novolac resins. Novolacs require use of hardeners and do not form cross-linked bonds (Marra1992).

Resins also have a great impact on final OSB panel strength. Resin dispersion, distribution, bond-line thickness, and resin penetration impact final strength of composite (White 1977, Ebewele 1979, White 1980, Shimizu 1981, Gagliano 2001). Ideal bond thickness varies for each species and resin used. Dispersion and distribution of resin is essential for quality wood bonding. Stress concentrations form around each resin droplet, as such care must be taken to

evenly distribute the small volume of resin used in OSB production. It is also important to add sufficient resin to prevent bond starvation, which results from penetration of resin into wood material (Marra 1992).

In wood composites, decreasing particle size (lumber → veneer → strand → flake → particle → fiber) results in decreased composite strength, if density is held constant. This is partially a result of fiber orientation, which becomes more difficult to control with decreasing particle size. However, composites from smaller dimension components exhibit greater dimensional stability, more isotropic mechanical properties, and greater uniformity (Bodig 1982, Marra 1992).

Increasing resin content of composite wood products increases the end product strength. However, the relationship is not linear and strength gains from increased resin content reach a maximum at 5%. After this point additional resin may in fact decrease strength of composite (Maloney 1977, Barnes 1981).

Increasing strand length increases mechanical properties of composites (Klauditz 1952, Page 1960, Stoffko 1960, Maloney 1977, Simpson 1977, Kyanka 1980, Higgins 1990). Increasing slenderness ratio (the ratio of strand length to thickness) increases modulus of elasticity, modulus of rupture, and tensile strength in strand based composites.

Thicker strands create stress riser effect or higher stress transfer angles between layers within OSB composite. This results in reduced strength if other parameters remain constant. OSB panels with longer and thinner strands, thus fewer stress transfer regions, show higher strength. Thicker strands create concentrated shear stresses at the ends of bonded flakes. Thicker strands may also interfere with bond formation, creating stresses that may create product defects and reduced strength (Marra 1992, Barnes 2001).

Alignment of strands within OSB also affects strength characteristics. Similar to the effect of grain angle on a piece of solid wood, misalignment of strands within OSB can reduce strength considerably with minimum deviation from parallel to long axis of panel (Chen 2007, Barnes 2000, Barnes 2001).

From an engineering standpoint, OSB in use (as sheathing in construction) acts as a shallow beam, with surfaces providing moment capacity and the core resisting shear forces. As with any member subjected to bending stresses it can be assumed the bending properties of a layered board are determined by the combined reaction of tension and compression stresses in bottom and top surfaces respectively (Beer 1981). Thus, panel surfaces have been estimated to contribute nearly 80% of MOE (Geimer 1979, Chen 2007).

Panels with denser strands on surface layers compared to core layer have been shown to exceed strength of panels without such distribution (Wang 2000). This concept is referred to as vertical density profile, VDP. Pressing of panels creates a density profile by compressing, and increasing density, of surfaces to greater extent than core material. Altering press closing rate, press temperature, and surface strand characteristics such as moisture content can cause considerable changes to VDP, impacting strength of panel (Suchsland 1974, Jin 2009).

Since OSB panels, and other wood composites, act under loading as simple beams strength can be modeled using derivation of existing mechanics equations. OSB strength, as previously mentioned, is sensitive to angle of stress, strand slenderness ratio, wood density, and final product density. Strength of OSB panels can be predicted based on strand strength characteristics by the following (Barnes 2001):

Equation 2.3 Barnes Model of wood composite strength in terms of flake characteristics (Barnes 2001)

$$\sigma_R = \frac{\sigma_{\parallel} \times \sigma_{\perp}}{\sigma_{\parallel} sin^n[\arctan(2t_b/l)] + \sigma_{\perp} cos^n[\arctan(2t_b/l)]}$$

$$t_b = t_a \times \left(\frac{\rho_a}{\rho_b}\right)$$

σ_R = *resultant strength* (*psi*)

$\sigma_{\parallel}$ = *strength parallel to the grain* (*psi*)

$\sigma_{\perp}$ = *strength perpendicular to grain* (*psi*)

n = *experimentally determined coefficient* (0.9 *to* 1.5)

l = *length of strand* (*in*)

t_a = *initial strand thickness* (*in*)

t_b = *in situ strand thickness* (*in*)

ρ_a = *initial wood density* (lb/ft^3)

ρ_b = *product wood density* (lb/ft^3)

2.6 References

Andre, N., Labbe, N., Rials, T., & Kelley, S. (2006). Assessment Of Wood Load Condition By Near Infrared (NIR) Spectroscopy. *JOURNAL OF MATERIALS SCIENCE*, *41*(7), 1879-1886. Doi: 10.1007/S10853-006-4433-6.

ASTM. (2000). Annual book of ASTM Standards. Section, 4.

Axrup, L., Markides, K., & Nilsson, T. (2000). Using Miniature Diode Array NIR Spectrometers For Analysing Wood Chips And Bark Samples In Motion. *Journal Of Chemometrics*, *14*(5-6), 561-572. Doi: 10.1002/1099-128X(200009/12)14:5/6<561::AID-CEM608>3.0.CO;2-2.

Barnes, D. (1981). Products of converted lignocellulosic materials. US Patent No RE30,636.

Barnes, D. (2000). An Integrated Model Of The Effect Of Processing Parameters On The Strength Properties Of Oriented Strand Wood Products. *FOREST PRODUCTS JOURNAL*, *50*(11-12), 33-42.

Barnes, D. (2001). An Integrated Model Of The Effect Of Processing Parameters On The Strength Properties Of Oriented Strand Wood Products (Vol 50, Pg 33, 2000). *FOREST PRODUCTS JOURNAL*, *51*(3), 7-7.

Beer, F., Russell, J., & Dewolf, J. (1981). *Mechanics Of Materials*. Mcgraw Hill.

Bendtsen, B. (1978). Properties of wood from improved and intensively managed trees. *Forest Products Journal*, *28*(10), 61-72.

Benson, P. (1930) The application of silviculture in controlling the specific gravity of wood. Technical bulletin (United States. Dept. of Agriculture)no. 168

Biblis, E., Carino, H., Brinker, R., & Mckee, C. (1995). Effect of stand density on flexural properties of lumber from 2 35-year-old loblolly-pine plantations. *Wood and Fiber Science*, *27*(1), 25-33.

Bodig, J., & Goodman, J. R. (1973). Prediction Of Elastic Parameters For Wood. *Wood Sci*, *5*(4), 249–264.

Bodig, J., & Jayne, B. A. (1982). Mechanics Of Wood And Wood Composites. *Van Nostrand Reinhold Co., New York, NY*, *7*, 12.

Chen, S., Fang, L., Liu, X., & Wellwood, R. (2008). Effect Of Mat Structure On Modulus Of Elasticity Of Oriented Strandboard. *WOOD SCIENCE AND TECHNOLOGY*, *42*(3), 197-210. Doi: 10.1007/S00226-007-0167-0.

Clouston, P., & Lam, F. (2001). Computational Modeling Of Strand-Based Wood Composites. *JOURNAL OF ENGINEERING MECHANICS-ASCE*, *127*(8), 844-851.

Conrad, M., Smith, G., & Fernlund, G. (2004). Fracture Of Wood Composites And Wood-Adhesive Joints: A Comparative Review. *WOOD AND FIBER SCIENCE*, *36*(1), 26-39.

Denne, M. P. (1989). Definition Of Latewood According To Mork (1928). *IAWA Bull. Ns*, *10*(1), 59–62.

Ebewele, R., River, B., & Koutsky, J. (1979). Tapered double cantilever beam fracture tests of phenolic-wood adhesive joints. Part I. Development of specimen geometry; effects of bondline thickness, wood anisotropy and cure time on fracture energy. Wood Fiber, 11(3), 197–213.

Fridley, K. (2002). Wood And Wood-Based Materials: Current Status And Future Of A Structural Material. *JOURNAL OF MATERIALS IN CIVIL ENGINEERING*, *14*(2), 91-96. Doi: 10.1061/(ASCE)0899-1561(2002)14:2(91).

Fujimoto, T., Kurata, Y., Matsumoto, K., & Tsuchikawa, S. (2008). Application Of Near Infrared Spectroscopy For Estimating Wood Mechanical Properties Of Small Clear And Full Length Lumber Specimens. *JOURNAL OF NEAR INFRARED SPECTROSCOPY*, *16*(6), 529-537. Doi: 10.1255/Jnirs.813.

Fujimoto, T., Yamamoto, H., & Tsuchikawa, S. (2007). Estimation Of Wood Stiffness And Strength Properties Of Hybrid Larch By Near-Infrared Spectroscopy. *APPLIED SPECTROSCOPY*, *61*(8), 882-888.

Gagliano, J. M., Frazier, C. E. (2001). Improvements in the fracture cleavage testing of a adhesively-bonded wood. Wood and fiber science, 33(3), 377–385.

Geimer, R. L. (1979). Data Basic To The Engineering Design Of Reconstituted Strandboard. In *Proceedings Of The 13t H Washington State University International Symposium On Particleboard* (Pp. 105–125).

Geimer, R. L., Montrey, H. M., & Lehmann, W. F. (1975). Effects Of Layer Characteristics On The Properties Of Three-Layer Particleboards. *Forest Prod. J*, *25*(3), 19–29.

Hankinson, R. L. (1921). Investigation of crushing strength of spruce at varying angles of grain. *Air Service Information Circular*, *259*.

Harris, J. M., B. A. Meylan. (1965). The influence of microfibril angle on longitudinal and tangential shrinkage in *Pinus radiata*. *Holzforschung*. 19:144–153.

Haygreen, J. G., & Bowyer, J. L. (1996). *Forest Products And Wood Science: An Introduction*. Iowa State University Press Ames.

Higgins, ED (1990). The strength of bonded wood strand composites. Thesis in the faculty of harvesting and wood science, Univ of British Columbia, Canada. 82-85.

Hoffmeyer, P., & Pedersen, J. G. (1995). Evaluation Of Density And Strength Of Norway Spruce Wood By Near Infrared Reflectance Spectroscopy. *Holz Als Roh-Und Werkstoff*, *53*(1), 165–170.

Jin, J., Dai, C., Hsu, W., & Yu, C. (2009). Properties Of Strand Boards With Uniform And Conventional Vertical Density Profiles. *Wood Science And Technology*, *43*(7), 559-574. Doi: 10.1007/S00226-009-0248-3.

Jones, P. D., Schimleck, L. R., Peter, G. F., Daniels, R. F., & Clark Iii, A. (2005). Nondestructive Estimation Of Pinus Taeda L. Wood Properties For Samples From A Wide Range Of Sites In Georgia. *Canadian Journal Of Forest Research*, *35*(1), 85–92.

Jones, P. D., Schimleck, L. R., Peter, G. F., Daniels, R. F., & Clark, A. (2006). Nondestructive Estimation Of Wood Chemical Composition Of Sections Of Radial Wood Strips By Diffuse Reflectance Near Infrared Spectroscopy. *Wood Science And Technology*, *40*(8), 709–720.

Kelley, S. S., Rials, T. G., Groom, L. R., & So, C. L. (2004). Use Of Near Infrared Spectroscopy To Predict The Mechanical Properties Of Six Softwoods. *Holzforschung*, *58*(3), 252–260.

Kelley, S. S., Rials, T. G., Snell, R., Groom, L. H., & Sluiter, A. (2004). Use Of Near Infrared Spectroscopy To Measure The Chemical And Mechanical Properties Of Solid Wood. *Wood Science And Technology*, *38*(4), 257–276.

Klauditz, W. 1952. Investigations on the suitability of various wood species, especially red beech wood, for the production of wood-chip boards. Report 25/52. Wood Research Institute, Braunschweig, Germany.

Kollmann, F. F., & Cote, W. A. (1968). Principles Of Wood Science And Technology, Vol. I: Solid Wood. *Principles Of Wood Science And Technology*, *1*.

Kruse, K., Dai, C., & Pielasch, A. (2000). An Analysis Of Strand And Horizontal Density Distributions In Oriented Strand Board (OSB). *Holz Als Roh-Und Werkstoff*, *58*(4), 270–277.

Kyanka, G. (1980). Fatigue Properties Of Wood And Wood Composites. *International Journal Of Fracture*, *16*(6), 609-616. Doi: 10.1007/BF02265220.

Lestander, T. A., Lindeberg, J., Eriksson, D., & Bergsten, U. (2008). Prediction Of Pinus Sylvestris Clear-Wood Properties Using NIR Spectroscopy And Biorthogonal Partial Least Squares Regression. *Canadian Journal Of Forest Research*, *38*(7), 2052–2062.

Mackerle, J. (2005). Finite Element Analyses In Wood Research: A Bibliography. *Wood Science And Technology*, *39*(7), 579–600.

Maloney, T. (1977). Modern particleboard and dry-process fiberboard manufacturing. Miller Freeman Publication. Inc., San Fransico, Calif, 94105.

Mark, R. E. (1980). Molecular And Cell Wall Structure Of Wood. *Journal Of Educational Modules For Materials Science And Engineering*, *2*.

Marklund, A., Hauksson, J. B., Edlund, U., & Sjoestroem, M. (1999). Prediction Of Strength Parameters For Softwood Kraft Pulps. Multivariate Data Analysis Based On Orthogonal Signal Correction And Near Infrared Spectroscopy. *Nordic Pulp And Paper Research Journal*, *14*, 140–148.

Markwardt, L. J., & Wilson, T. R. C. (1935). Strength And Related Properties Of Woods Grown In The United States.

Marra, A. A. (1992). *Technology Of Wood Bonding: Principles In Practice*. Van Nostrand Reinhold Company.

Neter, J., Wasserman, W., Kutner, M. H., & Others. (1985). *Applied Linear Statistical Models*. Irwin Burr Ridge, Illinois.

Page, D. H. (1969). A theory for the tensile strength of paper. Tappi, 52(4), 674–681.

Panshin, A. J., De Zeeuw, C., & Brown, H. P. (1970). *Textbook Of Wood Technology*. Mcgraw-Hill New York.

Paul, B. H. (1963). The application of silviculture in controlling the specific gravity of wood.

Record, S. J. (1914). The Mechanical Properties Of Wood. *John Wuey & Sons*.

Saliklis, E. P., & Mussen, A. L. (2000). Investigating The Buckling Behavior Of OSB Panels. *Wood And Fiber Science*, *32*(3), 259–268.

Schimleck, L. R., Wright, P. J., Michell, A. J., & Wallis, A. F. A. (1997). Near-Infrared Spectra And Chemical Compositions Of E. Globulus And E. Nitens Plantation Woods. *Appita Journal*, *50*(1), 40–46.

Schimleck, L. R., & Evans, R. (2002). Estimation Of Microfibril Angle Of Increment Cores By Near Infrared Spectroscopy. *IAWA JOURNAL*, *23*(3), 225–234.

Schimleck, L. R., Jones, P. D., Peter, G. F., Daniels, R. F., & Clarkiii, A. (2004). Nondestructive Estimation Of Tracheid Length From Sections Of Radial Wood Strips By Near Infrared Spectroscopy. *Holzforschung*, *58*(4), 375–381.

Schimleck, L. R., Jones, P. D., Clark, A. I., Daniels, R. F., & Peter, G. F. (2005). Near Infrared Spectroscopy For The Nondestructive Estimation Of Clear Wood Properties Of Pinus Taeda L. From The Southern United States. *Forest Products Journal*, *55*(12), 21–28.

Shimizu, S., Okuma, M. (1981). Fundamental studies on the strength of the oriented particleboard: on the bonding strength between wood particles. *Journal Of The Japan Wood Research Society, (27)1:8-13.*

Simpson, W. T. (1977). Model for tensile strength of oriented flakeboard. Wood Science 10(2):68-71.

Smith, I., Snow, M., Asiz, A., & Vasic, S. (2007). Failure Mechanisms In Wood-Based Materials: A Review Of Discrete, Continuum, And Hybrid Finite-Element Representations. *Holzforschung*, *61*(4), 352–359.

Stoffko, J. (1960). The relationship between the dimensions and geometry of wood particles and the mechanical properties of wood-particle boards. Drearsky Vyskum 5(1):241-261.

Suchsland, O., & Woodson, G. (N.D.). Effect Of Press Cycle Variables On Density Gradient Of Medium Density Fiberboard. In *Proceeding* (Vol. 8, Pp. 375–396).

Thumm, A., & Meder, R. (2001). Stiffness Prediction Of Radiata Pine Clearwood Test Pieces Using Near Infrared Spectroscopy. *Journal Of Near Infrared Spectroscopy*, *9*, 117.

Tsai, S. W. (1968). Strength theories of filamentary structures. Fundamental aspects of fiber reinforced plastic composites, 3–11.

Tsuchikawa, S., Hirashima, Y., Sasaki, Y., & Ando, K. (2005). Near-Infrared Spectroscopic Study Of The Physical And Mechanical Properties Of Wood With Meso-And Micro-Scale Anatomical Observation. *Applied Spectroscopy*, *59*(1), 86–93.

Tsuchikawa, S., Torii, M., & Tsutsumi, S. (1996). Application Of Near Infrared Spectrophotometry To Wood IV. Calibration Equations For Moisture Content. *Journal Of The Japan Wood Research Society*, *42*(8), 743–754.

Tsuchikawa, S., Torii, M., & Tsutsumi, S. (1997). Application Of Near Infrared Spectrophotometry To Wood V. Calibration Equations For Physical Conditions Of Wood. *Journal Of The Japan Wood Research Society*, *43*(8), 149–158.

US FPL (1974). Wood Handbook: Wood As An Engineering Material.

US FPL (2010). Wood Handbook: Wood As An Engineering Material.

Via, B. K., Shupe, T. F., Groom, L. H., Stine, M., & So, C. L. (2003). Multivariate Modelling Of Density, Strength And Stiffness From Near Infrared Spectra For Mature, Juvenile And Pith Wood Of Longleaf Pine (Pinus Palustris). *Journal Of Near Infrared Spectroscopy*, *11*(5), 365–378.

Via, B. K., So, C. L., Shupe, T. F., Groom, L. H., & Wikaira, J. (2009a). Mechanical Response Of Longleaf Pine To Variation In Microfibril Angle, Chemistry Associated Wavelengths, Density, And Radial Position. *Composites Part A*, *40*(1), 60–66.

Via, B. K., So, C. L., Shupe, T. F., Groom, L. H., & Wikaira, J. (2009b). Mechanical Response Of Longleaf Pine To Variation In Microfibril Angle, Chemistry Associated Wavelengths, Density, And Radial Position. *Composites Part A*, *40*(1), 60–66.

Via, B. K., So, C. L., Shupe, T. F., Stine, M., & Groom, L. H. (2005). Ability Of Near Infrared Spectroscopy To Monitor Air-Dry Density Distribution And Variation Of Wood. *Wood And Fiber Science*, *37*(3), 394–402.

Via, B. K., So, C., Shupe, T. F., Eckhardt, L. G., Stine, M., & Groom, L. H. (2005). Prediction Of Wood Mechanical And Chemical Properties In The Presence And Absence Of Blue Stain Using Two Near Infrared Instruments. *Journal Of Near Infrared Spectroscopy*, *13*(4), 201.

Wangaard, F. F. (1950). The Mechanical Properties Of Wood. *New York*.

Wangaard, F. F., & Zumwalt, E. V. (1949). Some Strength Properties Of Second-Growth Douglas Fir. *Journal Of Forestry*, *47*(1), 18–24.

Wellwood, R. W. (1962). *Tensile testing of small wood samples*. University of British Columbia, Faculty of Forestry.

White, M. S. (1977). Influence of resin penetration on the fracture toughness of wood adhesive bonds. Wood Science, 10(1), 6–14.

White, M., & Green, D. (1980). Effects of substrate on the fracture toughness of wood-adhesive bonds. Wood Science, 12(3), 149–153.

Chapter 3

Mechanical Testing Of Wood Strands: The Effect of Gage Length, Loading Rate, And Geometry

3.1 Introduction

3.1.1 Mechanical Testing Standards

Engineered wood composites have gradually, and in some cases rapidly, been incorporated into standard building practices in North America. The diminished availability of large timber has opened the door for composites that utilize wood particles from small diameter trees. Oriented strandboard (OSB) is an example of an engineering wood composite to successfully enter the forest products marketplace. Since introduction over 30 years ago OSB production volume has outpaced that of plywood in the United States and Canada. As a result, OSB production and consumption has surpassed plywood and today OSB dominates, holding 75% of structural panel market (Najera & Spelter 2001). Projections show that by 2020 OSB consumption in the US will exceed 2.8 billion square meters, while plywood consumption is estimated to fall below 1 billion square meters (Haynes 2003). Furthermore, between 1977 and 2006 improvements in technology and processes have led to a decrease in input to output ratio for OSB resulting in better wood yield efficiency (Spelter et al. 2006). Wood yield in OSB production has increased due to improvements in drying and pressing processes as well as improvements in resin formulations and application. Wood yield was further improved due to more efficient stranding operations in which longer strands could be cut while maintaining the thin dimension (Spelter et al. 2006).

Despite improvements in manufacturing efficiency, all wood strands in a production environment are treated as a bulk material resulting in strands that grossly under or over perform internal specifications due to processing defects, manufacturing variation, and wood quality. The feedstock quality varies both within and between trees resulting in strands that vary greatly in density, stiffness, and strength. The stranding process introduces defects to some strands resulting in end checking and longitudinal splits, both of which reduce the strength and stiffness of wood strands (Geimer et al. 1985). As a result, the quality of wood composite can decrease given the strong relationship between strand and composite quality (Deomano & Zink-Sharp 2004). Despite this relationship, there is a gap in current engineering models due to a lack of information on strand mechanical property values. Without the proper design values for wood strands, it is impossible to build engineering models or accurately predict the mechanical properties of strand-based composites (Lee 2003). It is the goal of this research project to develop a testing protocol for wood strands under axial-tensile and flexural stress.

Standards for testing tensile strength and stiffness of wood samples in the parallel-to-grain direction have existed for some time for both small clear wood and wood composite panels (DIN 52188, ISO 3345, ASTM D1037). However, wood strands are much smaller in dimension and it is unknown if scaling down current standards to strand size is appropriate. For small clear samples, specimen dimensions are 25.40 cm in length, 5.08 cm in width, and a taper to 3.81cm to the middle of the specimen (Reference ASTM standard). The thickness of the specimen is 2.54cm, and a minimum grip length of 50.8 mm is required. Conversely, the average strand size for composite panels measure roughly 12.70 cm in length, 2.54 cm in width, and 0.10 cm thickness. This study will attempt to determine if the dimensions in the length and width direction can be scaled down for strand testing while maintaining a typical thickness that might

be inherited from the strander. It is anticipated that the determination of tensile stiffness and strength parallel to grain for small clear samples may differ between current methodologies for clear wood and wood strands.

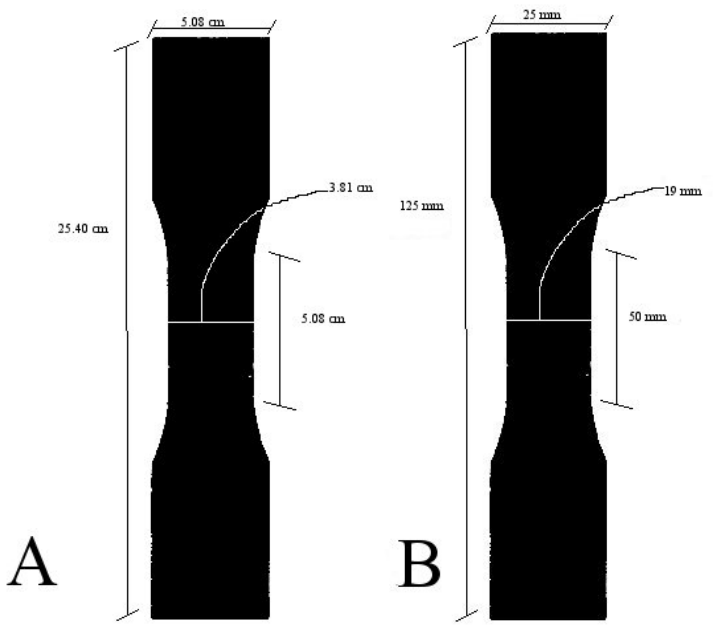

Figure 3.1 Schematic of wood strand sample that has been cut into a "dog-bone" shaped specimen (A. ASTM D1037, B. Bone sample used in strand tests)

The ASTM standard calls for a tensile sample that is bone shaped in which the sample gradually gets smaller in cross-sectional area from the edge to center (Figure 3.1) (ASTM D1037 2004). The reasons for utilizing a bone shaped tensile specimen are to lower the ultimate force at failure, to concentrate failure in a specific area, and to minimize hidden defects in the sample. A gradual taper allows for a smooth transition of load distribution from the edge to the center so as to remove the possibility for a stress concentration (Kretschmann 2008) Furthermore, the small cross sectional area allows for small loads to failure which is important since wood is strongest in tension parallel to the grain (FPL 1999), and minimizing the maximum force exerted through a smaller cross sectional area can help to minimize slippage in the grips. To reduce the effects of compressive forces at the grips, it is essential to concentrate failure in the mid-section of the

sample to accurately determine tensile strength. The concept draws on Saint-Venant's principle: localized effects caused by any load acting on the body will dissipate or smooth out within regions that are sufficiently away from the location of the load. (Timoshenko 1953). Thus fractures in the center of tensile sample can be assumed to be the result of axial strain alone, and not appreciably influenced by the compressive forces acting on the sample ends.

When testing wood strands in tension parallel–to-grain, there are reasonable justifications for going to a rectangular shape. First, the cross sectional area of a wood strand is sufficiently small without tapering and allows for easier measurement of tensile testing. Second, the small cross sectional area does not allow for hidden defects (knots, pith, checking) common in larger wood samples. Finally, machining wood strands into bone geometries without damaging the strand can be difficult, particularly for strands from a manufacturing process.

To date, the use of bone geometry in wood strand tensile testing has not been investigated. A summary of tensile testing literature regarding wood strands is presented in Table 3.1 The primary goal of this research is to investigate the effect of sample geometry (bone versus rectangle) on tensile properties for strands in which the grain is parallel to the sample axis. After geometry is chosen, the gage length and loading rate will be verified to determine the best setup for testing.

3.1.2 Tensile Testing of Strands

Wood strands can be made from lumber such that laboratory prepared samples are available for research and development purposes or strands can come from a manufacturing process in which grain angle, defect occurrence and defect type can vary. Methods to test either scenario would be useful but currently there are no ASTM standards for wood strands. Table 3.1

provides a summary of significant research performed on strands and demonstrates there is a lack of understanding about testing wood strands that have been prepared into a "dog-bone" shape.

Table 3.1 Summary Wood Strand Tensile Testing Literature

Tension Parallel to Grain	Gage Length (mm)	Thickness (mm)	Loading Rate (mm/min)	MOE 10^9 Pa	UTS 10^6 Pa	Species	Shape
Price (1976)	12.7/19.1/ 25.4/31.8 (6.35)	0.381	0.160	3.24/3.94/ 3.82/4.65	65.6/64.1/ 56.1/54.4	*Liquidambar styraciflua*	Rectangle
Geimer et al. (1985)	38.1	0.381	0.190	6.16/5.99	36.9/37.7	*Pseudotsuga menziesii*	Rectangle
Hunt (1989)	228.6 (152.4)	0.794	1.90	11.8	70.3	*Liriodendron tulipifera*	Rectangle
Wu et al. (2005)	152.4 (25.4)	0.38	0.127	12.84	49.98	*Pinus spp.*	Rectangle
Cai (2007)	152.4 (25.4)	0.508-1.27	0.127	8.60	58.7	*Pinus spp.*	Rectangle
				7.89	40.7	*Quercus spp.*	Rectangle
Hindman & Lee (2007)	40.0	0.66	0.127	4.91	43.3	*Pinus taeda*	Rectangle
Jeong et al. (2008)	102 (50.8)	0.381/0.794 /1.91/3.81	0.254	11.4/12.9/ 13.5/2.14	37.3/47.2/ 46.0/73.8	*Pinus spp.*	Rectangle
	extensometer or strain gage length in ()						

Significant research has been conducted on tensile properties of individual wood growth zones. However, this early research was conducted by machining standard tensile test specimens' center section to a single growth ring or growth zone (ASTM D143, Wellwood 1962, Biblis 1969). Due to the initial size of a wood strands, it is impossible to use ASTM D143 as a starting point for tensile tests.

Price (1976) was the first to test the mechanical properties of wood strands prior to composite manufacture. Price (1976) evaluated the bending strength and stiffness of sweetgum (*Liquidambar styraciflua*) flakes before and after pressing into flakeboard panels. The dimensions of flakes tested were 76.2 mm in length, 9.5 mm in width, and 0.38 mm in thickness.

Flakes were conditioned at 22°C (72°F) and 50% relative humidity. The slope of grain was measured from the longitudinal-tangential plane and used to adjust mechanical properties through covariance analysis. Price used a strain rate of 0.127 mm/mm/min as this was and is the ASTM strain rate for panel flexural tests (ASTM 2004). Flakes were loaded to failure. Price did not use bone geometry and tested at gage lengths of 12.7mm, 19.1mm, 25.4mm, and 31.8mm. An electrical resistance strain gauge 6.35mm long was used in conjunction with recorded crosshead movement. To limit slippage, 620kPa (90lb/in^2) force was applied at the grips which were lined with 50-grit sandpaper. Despite these efforts Price did observe some slippage at the grips and found better results with the electrical resistance strain gage based on comparisons with tensile strength and stiffness of solid sweetgum reported by the Forest Products Laboratory (US FPL 1999). Based on these comparisons and ease of manipulation, Price used a 19.1 mm gage length for remainder of research comparing flake strength before and after hot pressing.

In 1985 Geimer et al. investigated the influence of processing damage on strength of Douglas-fir (*Pseudotsuga menziesii*) flakes. To achieve this, two grades of flakes were utilized. Grade A flakes were cut from rough sawn lumber using a disk flaker with sharpened blades. Grade B flakes were cut from the same material but with dulled blades in the disk flaker. Flakes were conditioned at 21°C (70°F) and 66% relative humidity. Flakes were cut to 88.9 mm in length, 12.7 mm width, and 0.38 mm thickness. The flakes tested were not cut into bone shape but were trimmed to aforementioned dimensions prior to testing. Tensile testing was conducted at 0.127 mm/min loading rate to failure in an environmentally controlled room. The gage length was 38.1mm and crosshead movement was used to record strain. Pneumatically controlled grips were used and 4137 kPa (600lb/in^2) pressure was applied. Slippage was not reported but it is

possible some slippage occurred but could not be reported as an extensometer or strain gauge was not used to confirm strain.

The previous studies were conducted on flakes used in flakeboard. Flakeboard was the precursor to oriented strandboard and was often produced in plants with three-pass type dryers that could only handle shorter flakes (~90mm). As strandboard production increased in the late 1970s, plants adopted dryers and conveyors which could handle flakes of roughly 150mm length, called strands. Strands of various lengths over 127mm are utilized in both oriented strandboard panels and parallel wood strand composite boards.

As part of a project to predict strength and stiffness of parallel strand composites, the tensile properties of yellow-poplar (*Lirodendron tulipifera*) were investigated (Hunt 1989). Yellow-poplar veneer sheets were used in the research after conditioning at 22°C (72°F) and 36% relative humidity. Strands were initially cut into 101.6cm by 1.27cm strands and then clipped to 30.48cm length before equilibration. A semi-automated computer-aided measurement system was used to measure thickness and width at 3 sections along the 30.48 cm length. The average of the measurement was used for all calculations. Samples were then tested using a custom tensile testing machine with 228.6 mm gage length and 152.4 mm extensometer gage length. Grips were hydraulically controlled though no clamping pressure was recorded. The grips were not serrated or coated in sandpaper but instead faced with rigid urethane. Strands were loaded at 1.9 mm/min crosshead movement to a load of 222.4 N. Other strands were loaded to failure to determine ultimate tensile strength (UTS). Tensile modulus of elasticity (MOE) was determined by linear regression from 44.48 to 222.4 N. Hunt noted that 15% of samples had to be rejected due to failure at the grip region of the specimens.

Later, research was published investigating tensile and dimensional properties of wood strands exposed to pressing and resin conditions (Wu et al. 2005). This research was conducted in Louisiana and plantation grown southern yellow pine (*Pinus spp*.) strands were used. Strands were cut from veneers to 152.4mm length, 25.4mm width, and average thickness of 3.8mm. Strands were sorted into three groups for high, medium, and low annual ring count (ARC) per 2.54 cm. In all 240 strands were tested. Strands were equilibrated to approximately 11% moisture content prior to testing. Mechanical testing for tensile modulus and strength was conducted using a MTS load frame with matching MTS extensometer and hydraulic grips. Extensometer gage length was 25.4mm, and total strand length was 152.4mm (clamping length was not mentioned). A loading rate of 0.127 mm/min was used. Modulus of elasticity was calculated according to ASTM standards, allowing either regression along the straight portion of the stress-strain curve or secant along any straight portion in stress-strain curves lacking initial straight-line from origin.

Mechanical properties of wood strands were once again investigated for the effect of hot-pressing and resin application on strand properties (Cai 2007). This research investigated the mechanical properties of four species found in Louisiana: red oak (*Quercus spp.*), willow (*Salix spp.*), yellow-poplar (*Liriodendron tulipifera*), and loblolly pine (*Pinus taeda*) which is one of the four southern yellow pine species. Strands were cut using a 915 mm disc flaker. Strand dimensions were 152.4 mm length, 25.4 mm width, and the thickness was varied from 0.5 to1.27 mm. Strands were conditioned at 25℃ and 65% relative humidity. Mechanical testing for tensile modulus and strength was conducted using a MTS load frame with matching MTS extensometer and hydraulic grips. Extensometer gage length was 25.4mm and total strand length was 152.4 mm (clamping length was not mentioned). A loading rate of 0.127 mm/min was used.

MOE was calculated according to ASTM standards, allowing either regression along straight portion of stress-strain curve or secant along any straight portion in stress-strain curves lacking initial straight-line from the origin.

In 2007 research was published to examine the effect of intra-ring properties on both flexural and tensile properties of wood strands (Hindman & Lee 2007). The research utilized loblolly pine (*Pinus taeda*) strands measuring 152.0 mm in length, 25.4 mm width, and 0.66-0.68 mm in thickness. Tensile testing was conducted on 60 mm samples with a 40mm gage length (10mm length per grip). Ends were wrapped in sandpaper prior to clamping in grooved grips. Loading rate used was 0.127 mm/min and crosshead movement was used to measure deflection.

The latest published research on tensile testing of wood strands Jeong et al. specifically investigated effect of loading rate and thickness on wood strand tensile properties (Jeong et al. 2008). A disc flaker was used to cut strands from a single southern yellow pine (*Pinus spp.*) board. Samples were cut to 139.7 mm length, 25.4 mm width. Four thicknesses were cut: 0.381 mm, 0.794 mm, 1.91 mm, and 3.81 mm. Prior to tensile testing, samples were conditioned at 25.4℃ and 36% relative humidity, which correspond to an equilibrium moisture content of 7.0%. Samples of 0.794 mm thickness were measured at loading rate of 0.102 mm/min, 0.254 mm/min, and 0.406 mm/min. Other thicknesses were only tested at 0.254 mm/min. All samples were of rectangle geometry and tested over 102 mm gage length with a 50.8 mm extensometer gage length. The testing grips were pressure driven though no clamping pressure was provided. Based on findings, Jeong et al. recommended a loading rate of 0.254mm/min with thickness between 0.794 and 1.91mm when testing strands in tension parallel to grain.

Table 3.2 Summary Wood Strand Flexural Testing Literature

Flexural	Test Span (mm)	Loading Rate (mm/min)	MOE 10^9 Pa	MOR 10^6 Pa	L/d	Species
Deomano & Zink-Sharp (2004)	25.0	2.54	4.43	78.6	41.6	*Liquidambar styraciflua*
			5.83	89.0		*Liriodendron tulipifera*
			4.09	66.0		*Pinus spp.*
Hindman & Lee (2007)	18.11	0.127	5.78	89.2	26.6	*Pinus taeda*

Currently two publications have assessed flexural properties of wood strands; a summary of findings is presented in Table 3.2. In 2004, Deomano & Zink-Sharp investigated the flexural properties of three species commonly used for structural composites and panels. The species tested were yellow-poplar (*Liriodendron tulipifera*), sweetgum (*Liquidambar styraciflua*), and southern yellow pine (*Pinus spp.*). Using a disc flaker, strands of 0.6 mm thickness were prepared. The bending samples were 25.0 mm in length and 5.0 mm in width. Samples were tested at 2.54 mm/min loading rate in three-point bending on the flat side of the flake. In 2007 Hindman & Lee used 33.0mm long, 11.0mm wide, and 0.68mm thick strands for flatwise bending. Test span for tests was 18.11mm with 0.127mm/min loading rate.

Despite a reasonable level of research on strand-based composites, no standard for determining strand mechanical properties is available. Thus the aforementioned publications have utilized ASTM D1037, a standard for composite panel testing, as a basis for mechanical testing protocols. The wide variation in strand length, strand thickness, extensometer gage length, and loading rate make comparisons between studies difficult (see Table 3.1). Loading rate and gage length have been shown to affect apparent MOE and UTS (Price 1976). Furthermore, much of the existing research can only be applied to strands produced in a

laboratory setting, although Geimer et al. (1985) were able to test strands that are most similar to those produced in industry. In an industrial setting, such as oriented strandboard production, strands are cut to a target length of around 125 mm or less. A length less than 125 mm precludes many of the testing standards. Based on a 125 mm long strand, the maximum gage length available for tensile testing is around 75 mm if 50 mm is assumed to provide an adequate clamping length. It should be noted that multiple researchers: Price, Geimer et al., and Jeong et al. noted slippage of wood strand during tensile testing (Price 1976, Geimer et al. 1985, Jeong et al. 2008). Also, most researchers noted the tensile strength values for wood strands do not match the Wood Handbook values for solid wood. Geimer et al. (1985) attributed this reduction in strength to size reduction from solid sample and manufacturing defects observed in strands (Geimer et al. 1985). While using shorter gage lengths yielded results similar to Wood Handbook values for tensile strength, the FPL values could not be achieved (Price 1976, US FPL 1999).

Because strand mechanical properties have been shown to differ from solid wood properties, there is a need for development of a new standard for wood strands. An accurate understanding of strand mechanical performance is necessary if an accurate predictive or engineering model for strand composites is to be achieved. Furthermore, the latter portion of this research will be focused on utilizing near infrared spectroscopy for prediction of strand mechanical properties and NIR spectra based models with lower root mean square error is possible if the test protocol utilized for calibration data has better precision.

3.2 Materials and Methods

3.2.1 Preparation of Samples for Loading Rate versus Gage Length Testing

To determine the optimum loading rate and gage length, a population of matched strands was used to create homogeneous samples. The use of homogenous samples help to reduce the error associated to the experimental unit. Strands were cut from one southern red oak (*Quercus spp.*) end-matched veneer. Veneer was used to control inter-tree variation, annual ring count, density, and thickness. Veneer was quarter sliced ensuring all strands were radial faced. Strands were cut to 76.2 mm length, 25.4 mm width, and 0.85 mm thickness. Strands were cut from veneer using a guillotine paper cutter and visually-inspected for straightness of grain. Strands in each group were selected along longitudinal axis of the veneer to ensure homogeneity between samples and assumes that mechanical properties do not differ significantly from the same growth ring along longitudinal axis of tree (US FPL 1999, Via et al. 2009). If a section of veneer was damaged due to drying or peeling, no strands were cut from that region. Likewise any strands with splitting incurred during the cutting process were discarded. Bone shaped strands were made by first scaling ASTM bone testing dimensions from a length of 25.40 cm and a width of 5.08 cm tapering to 3.81cm) down to 125.0 mm length and 25.4 mm width . The bone shaped pattern was then traced onto the rectangular shaped sample with a pencil and the bone shaped sample was cut out using a razor blade. Samples damaged during this process were also discarded. Strands were conditioned at 22°C and 50% relative humidity. The strands were then tested at different gage lengths and loading rates. The experimental design can be seen in Table 3.3.

Table 3.3 Gage Length Vs Loading Rate Experimental Setup

n=60	Gage Length (mm)	Loading Rate (mm/min)	Species	Shape
A	50.8	0.254	*Quercus spp.*	Rectangle
B	25.4	0.254	*Quercus spp.*	Rectangle
C	50.8	0.127	*Quercus spp.*	Rectangle
D	76.2	0.127	*Quercus spp.*	Rectangle
E	76.2	0.254	*Quercus spp.*	Rectangle
F	76.2	0.254	*Quercus spp.*	Bone

3.2.2 Preparation of Bone and Rectangle Shaped Specimens from an Industrial Process

To determine the effect of bone geometry versus rectangle geometry on tension-parallel to-grain, strands produced by a commercial stranding operation at a local oriented strandboard plant were used. The strands tested were southern yellow pine (*Pinus spp.*) and were collected after the fines were screened from the furnish. Strands were sorted visually in the laboratory and any strands with end splitting or warpage were not included in the study. The target dimensions of sorted strands were 127 mm in length and 25 mm in width. Strand thickness varied due to the stranding process used at the plant, with an average of 0.85 mm. Strands were then sorted into groups by annual ring count (ARC). An ARC group was classified as being: “low” if the strands possessed only 1 complete ring per centimeter, “medium” if there were 2 complete rings per centimeter, and “high” if there were 3 or more rings per centimeter. Each annual ring count group was further split into two groups: one of rectangle geometry, one of bone geometry. Bone shaped strands were made by first scaling ASTM bone testing dimensions (length of 25.40 cm, width of 5.08 cm tapering to 3.81cm) to fit the 125.0mm length and 25.4mm width of strand. The pattern was then traced onto sample and cut out using razor blade. Samples damaged during

cutting of bone geometry were also discarded. Strands were conditioned at 22°C and 50% relative humidity. Table 3.4 shows experimental design for bone verusus rectangle tests.

Table 3.4 Bone Vs Rectangle Geometry Experimental Setup

n=91	Gage Length (mm)	Extensometer Gage Length (mm)	Loading Rate (mm/min)	ARC	Species	Shape
I	76.2	50.8	0.254	L	*Pinus spp.*	Rectangle
II	76.2	50.8	0.254	M	*Pinus spp.*	Rectangle
III	76.2	50.8	0.254	H	*Pinus spp.*	Rectangle
IV	76.2	50.8	0.254	L	*Pinus spp.*	Bone
V	76.2	50.8	0.254	M	*Pinus spp.*	Bone
VI	76.2	50.8	0.254	H	*Pinus spp.*	Bone

3.2.3 Preparation of Samples for Tension Testing

After establishing testing protocols, two more sets of wood strands were evaluated in tension parallel to the grain. The first set of flakes was collected from wood strands produced in a commercial stranding operation. All wood strands utilized were southern yellow pine (*Pinus spp*.). Plant strands were obtained from the Louisiana-Pacific Hanceville (Hanceville, AL) OSB plant and the methodology was similar to section 3.2.3 except for the fact that the flakes were collected from the manufacturing line before screening. Sawn strands were produced from cutoffs donated by Capitol Truss (Wetumpka, AL) and Dudley Lumber Co (Salem, AL), and boards purchased locally. Boards and cutoffs were cut into clear samples (25 mm by 25 mm by

200 m in length) and placed in a humidity chamber, at 22°C and 50% relative humidity, until processing began.

Plant strands to be used during experimentation were sorted from approximately 1.3 cubic meters of unscreened strands. Radially-cut strands with dimensions of greater than 125 mm in length and 25mm in width were selected. Strands with splitting or warp (bends, twists, cupping) were not selected. The selected strands were then cut to uniform size using a guillotine paper cutter.

To produce sawn strands, the collected lumber cutoffs were first cut into small clear samples measuring 200 x 25 x 25 mm. These small clear samples were then ripped along the radial face to produce strands of approximately 200 x 25 x 1.0 mm. Prior to testing the strands were cut to 125 mm in length to facilitate mounting in grips. Both plant and sawn strands were conditioned at 22°C and 50% relative humidity.

3.2.4 Mechanical Testing of Strands

For flexural testing, loading rates between 0.102 mm/min to 0.406 mm/min have been researched for both composite panels and strands (Price 1976, Wu 2005, Cai 2007, Hindman & Lee 2007, Jeong et al. 2008). Other researchers have used gage lengths from 12.7mm to over 200mm (Table 3.1). The gage length used is limited by the testing load frame, extensometer or strain gauge size, and material dimensions. In this case the strand length was 125 mm, with50 mm required for clamping in the grips (25.4 mm each end). The maximum gage length (grip-to-grip separation) for testing was 76.2mm.

Axial tension tests were conducted using a Zwick-Roell load frame equipped with 10 kN load cell and computer controlled screw-drive crosshead (Figure 3.2 c). Screw type grips were

used. According to the manufacturer, such grips are of sufficient clamping power for use with thin films and metals, and would be sufficient for wood strand application. Sandpaper or other abrasive was not used in grips as the clamping jaw surface was serrated to reduce slippage. It is also noted that the serrated grips were removable and new at time of study.

For initial loading rate and gage rate tests machine gage lengths (grip-to-grip separation) of 25.4 mm, 50.8 mm, and 76.2 mm were used, with loading rates of 0.127 mm/min and 0.254 mm/min. For test of bone geometry versus rectangle geometry, a clip-on extensometer with a gage length of 50.8 mm (Epsilon Corp.) was used. Extensometer calibration was tested by attaching to a split flake and loading at 0.254 mm/min. Verification was performed in which the extensometer travel matched the crosshead travel through the extensometer range.

Flexural tests were conducted in three-point setup with loading rate of 4.0 mm/min, and support separation of 75 mm for sawn strands and 50 mm for plant strands (Figure 3.2 a-b). Rounded supports and load head of 5 mm radius were used in accordance with ASTM standards which dictate that the radius must be greater 1 ½ times the thickness of the material when tested in bending (ASTM 2004).

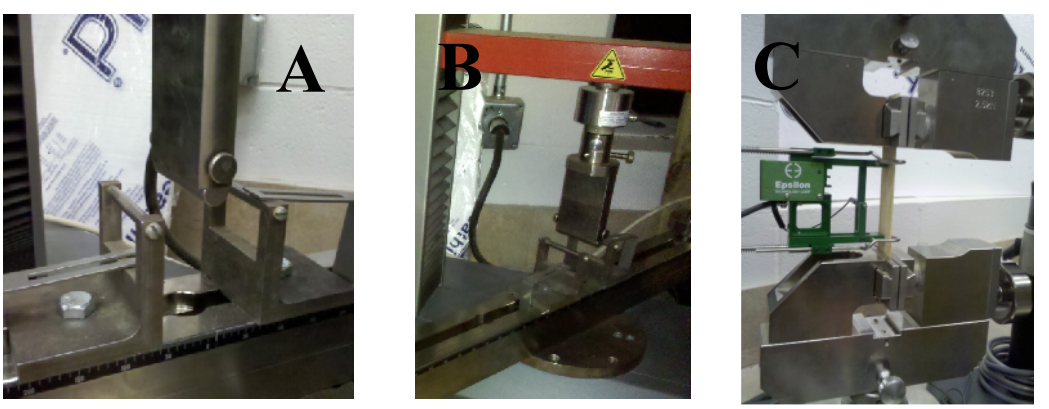

Figure 3.2 Mechanical Testing Setups: Flexural Testing (Close Up) (A), Flexural Testing (With Load Cell) (B), Tensile Testing (C)

3.3 Results and Discussion

3.3.1 Tensile Results

As expected, increasing the gage length resulted in an increase in tensile modulus (Rosen 1967, Price 1976). The 76.2 mm gage length had the highest measured tensile MOE. On the other hand, tensile strength is expected to decrease (Price 1976) with increasing gage length. This was not entirely the case as the shorter gage lengths (25.4mm, 50.8mm) were more likely to exhibit fractures extending through the grips. Within a gage length group, increases in loading rate were accompanied by increases in tensile MOE. Increasing loading rate also increased measured UTS. This observation can be attributed to the viscoelastic nature of wood. The measured UTS for rectangle samples averaged 26.64 MPa, which is only 23.8% of the published values for UTS of red oak (*Quercus spp.*) (US FPL 1999). This reduction in UTS has been the observation of numerous researchers testing wood strand mechanical properties (Price 1976, Geimer et al. 1985, Hunt 1989, Jeong et al. 2008). The UTS of bone shaped samples was much higher and approximately 67.8% of the 112MPa value recorded in the Wood Handbook (US FPL 1999).

Table 3.5 Gage Length Vs Loading Rate Experimental Results for *Quercus spp*.

n=60	Gage Length (mm)	Loading Rate (mm/min)	MOE 10^9 Pa (COV)	UTS 10^6 Pa (COV)	Species	Shape
A	25.4	0.254	3.68 (4.1)	33.68 (11.6)	*Quercus spp.*	Rectangle
B	50.8	0.254	5.96 (3.2)	31.43 (14.6)	*Quercus spp.*	Rectangle
C	50.8	0.127	4.95 (8.9)	26.93 (25.6)	*Quercus spp.*	Rectangle
D	76.2	0.127	6.48 (7.6)	25.62 (16.3)	*Quercus spp.*	Rectangle
E	76.2	0.254	8.00 (4.6)	46.33 (23.5)	*Quercus spp.*	Rectangle
F	76.2	0.254	11.44 (15.9)	75.98 (19.3)	*Quercus spp.*	Bone

The coefficient of variation also varied between gage lengths and loading rates. Although no trend for coefficient of variation for MOE was observed with increasing gage length, increased loading rate resulted in a decrease in COV. The same trend was not observed in the analysis of UTS. Increasing gage length resulted in increased COV for UTS. The lowest COV for tensile modulus (3.2%) was obtained with 50.8 mm gage length and 0.254 mm/min loading rate. The lowest COV for UTS (11.6%) was obtained with 25.4 mm gage length and 0.254 mm/min loading rate. However, these testing parameters also resulted in more samples being rejected due to grip failures. According to the US FPL, which provides research on tensile strength values but not tensile modulus, a UTS COV of 25% is considered acceptable for solid wood samples tested in tension parallel to the grain (US FPL 1999). The lower COV's in this study were especially notable considering the fact that smaller samples are expected to vary more than larger samples due to the increased influence of a single latewood or earlywood ring. The testing setup with 76.2 mm gage length and 0.254 mm/min loading rate was chosen for future testing, which is in agreement with the recommendations of Jeong et al. (2008) (Table 3.1). This

was recommended as the optimum combination in this study because it provided a low COV for both MOE (4.6%) and UTS (23.5%), and fewer samples were rejected for grip failures compared to other test setups.

Table 3.6 Bone Vs Rectangle Geometry Experimental Results

n=91	Gage Length (mm)	Extensometer Gage Length (mm)	Loading Rate (mm/min)	ARC	MOE 10^9 Pa	UTS 10^6 Pa	Species	Shape
I	76.2	50.8	0.254	L	2.93	24.57	*Pinus spp.*	Rectangle
II	76.2	50.8	0.254	M	3.79	26.53	*Pinus spp.*	Rectangle
III	76.2	50.8	0.254	H	5.45	30.70	*Pinus spp.*	Rectangle
IV	76.2	50.8	0.254	L	3.26	30.50	*Pinus spp.*	Bone
V	76.2	50.8	0.254	M	5.03	37.93	*Pinus spp.*	Bone
VI	76.2	50.8	0.254	H	5.71	38.12	*Pinus spp.*	Bone

ARC L-1 ring/cm M-2-3 ring/cm H-3+ ring/cm

Following tests tensile tests of rectangle and bone geometry samples, results were analyzed using SAS JMP 7.0 to perform Tukey-Kramer HSD. The analysis showed no significant difference ($p=0.005$) between MOE for the same ARC groups. However, it is clear that using bone geometry increases recorded MOE and UTS. The combination of high ARC and bone geometry showed a significant difference in UTS when compared to the low ARC and rectangle geometry treatment UTS. For MOE, there was no statistical difference between samples of low and medium annual ring count. High annual ring count specimens were significantly different in MOE from all other samples tested and were a reflection of the importance of latewood percentage on specimen stiffness. Thus it was concluded that bone

geometry does not significantly affect measured MOE and UTS in tension, but ARC is a factor in testing which agrees with the findings of Wu et al. (2005).

3.3.2 Flexural Results

Preliminary flexural testing of strands was conducted to ensure COV values were below FPL recommended COV for flexural tests, 22% for MOE and 16% for MOR (US FPL 1999). A loading rate of 4.00mm/min was used based on ASTM D1037 (ASTM 2004). Based on preliminary results in Table 3.7, loading rate of 4.00mm/min was acceptable and would be used for flexural testing.

Table 3.7 Initial Flexural Testing

n=20	Test Span (mm)	Loading Rate (mm/min)	MOE 10^9 Pa (COV)	MOR 10^6 Pa (COV)	L/d	Species
Sawn Test Strands	75.0	4.00	3.88 (15.7)	87.4 (13.3)	42	*Pinus spp.*

Sample stiffness was calculated at length to thickness (L/d) ratio of 43 for comparison to existing literature on wood strand flexural properties. To do so Equation 3.1 was used. Sample stiffness was calculated using K_i of 1.2 for concentrated midspan load, a $\frac{16}{1}$ shear free modulus of elasticity (E) to modulus of rigidity (G) ratio, and at a span to depth (L/d) ratio of 42 for comparison to existing literature on wood strand flexural properties. With average strand thickness of 1mm, the shorter test span of 50mm ensured pure bending failure (L/d ratios under 14 may produce shear failure rather than bending moment failure, and will minimize deflections caused by shear deformations).

Equation 3.1 Standardization of apparent moduli for beams of different span-depth ratio (Hilbrand 1967)

$$E_{ai2} = \frac{1 + K_1\left(\frac{h_1}{L_1}\right)^2\left(\frac{E}{G}\right)}{1 + K_2\left(\frac{h_2}{L_2}\right)^2\left(\frac{E}{G}\right)} \cdot E_{ai}$$

The measured stiffness (tensile modulus) for sawn strands was considerably higher than that of plant strands as shown in Table 3.8. UTS was also much higher for sawn strands compared to plant strands. Furthermore, the calculated coefficient of variation for tensile modulus and UTS was much lower for the sawn strands compared to the plant strands. It is likely the discrepancy in stiffness and strength is due to splits, checks, and other defects incurred during stranding. The coefficient of variation of mechanical properties of plant strands was much higher than that of sawn strands. Sawn strands exhibited a UTS COV of 24.22%, which fell below the recommended limit of 25% established by the US FPL Wood Handbook. Geimer et al. reported similar coefficient of variation in both MOE (31.4%) and UTS (51.0%) (Geimer et al. 1985). UTS for plant strands was only 46% of published values for southern yellow pine parallel to grain (US FPL 1999). However, as Table 3.8 demonstrates, the UTS of sawn strands was very close to the reported value of 80MPA (US FPL 1999). It is also noteworthy to point out that the MOE results compared well to Jeong et al. (2008) values for tensile modulus of southern yellow pine strands. Typically failures occur in the latewood region due to combined tension and shear forces while failures in the earlywood region are brittle and occur across the tracheid walls (Bodig & Jayne 1982). Under the testing parameters used, most samples exhibited combined tension and shear failure mode

Table 3.8 Plant Strands Vs Sawn Strands Tensile Experimental Results

n=150	Gage Length (mm)	Extensometer Gage Length (mm)	Loading Rate (mm/min)	MOE 10^9 Pa (COV)	UTS 10^6 Pa (COV)	Shape	Species
Plant Strands	76.2	50.8	0.254	7.97 (36.72)	37.0 (41.11)	Rectangle	*Pinus spp.*
Sawn Strands	76.2	50.8	0.254	13.60 (29.78)	80.1 (24.22)	Rectangle	*Pinus spp.*

Table 3.9 shows results of flexural testing results. A shorter test span was used for the plant strands because of end splitting and warp. Like the tensile results, MOE was much higher for sawn strands compared to plant strands and the associated COV were also lower for sawn strands. Modulus of rupture was also higher for sawn strands and had a lower COV compared to plant strands. This is again attributed to defects in the plant strands incurred during stranding and handling. The average published modulus of rupture for small clear southern yellow pine samples is 90MPa (US FPL 1999) while the MOR of sawn strands in this study was similar at 92.61MPa average. However, the published MOE in bending for the four southern yellow pine species falls somewhere between 12 and 13GPa; the measured values for both sawn and plant strands is much lower. The US FPL Wood Handbook recommends, for solid wood samples, COV for MOE in flexural tests to be around 22% and 16% for MOR. Although neither group was below the FPL recommended COV for MOE or MOR, the COV were much lower for sawn strand tests (US FPL 1999).

Table 3.9 Plant Strands Vs Sawn Strands Flexural Experimental Results

n=100	Test Span (mm)	Loading Rate (mm/min)	MOE 10^9 Pa (COV)	MOR 10^6 Pa (COV)	L/d	Species
Plant Strands	50.0	4.00	3.04 (37.3)	54.06 (29.78)	43	*Pinus spp.*
Sawn Strands	75.0	4.00	4.41 (27.02)	92.61 (17.45)	43	*Pinus spp.*

Based on experimentation, testing parameters were developed for both tensile and flexural tests of small wood strands. For tensile testing, a gage length of 76.2mm, with a 50.8mm extensometer gage length, and loading rate of 0.254 mm/min is recommended. At this gage length and loading rate, there was sufficient clamping pressure in serrated grips to prevent slippage. Better testing results in terms of strength, stiffness, and coefficient of variation can be achieved by using prepared flakes in place of commercially produced strands.

Flexural testing of strands was much simpler than tensile testing because slippage at the grips was not a concern. Strand length variation (50 versus 75 mm) did not significantly influence the average or COV while a 4.0 mm/min loading rate yielded the lowest COV.

Plant strands exhibited mechanical properties that were lower than sawn strands. It is most likely that the reduction in strength is due to fiber damage and longitudinal fractures. As early as 1952 it was observed that small wood samples suffer strength reductions due to damage of individual fibers (Kloot 1952). When used in composites, such defects and strength reductions are probably not of consequence due to resin spot welding (Geimer et al. 1985), but for accuracy in mechanical testing only prepared strands should be used

3.4 References

ASTM. (2004). Annual book of ASTM Standards. Section, 4.

Beer, F., Russell, J., & Dewolf, J. (1981). *Mechanics Of Materials*. Mcgraw Hill.

Biblis, E.J. (1970). Tensile properties of loblolly pine growth zones. Wood and Fiber Science.1(1):18-28.

Bodig, J., & Jayne, B. A. (1982). Mechanics Of Wood And Wood Composites. *Van Nostrand Reinhold Co., New York, NY*, *7*, 12.

DIN 52188 (2009). Wood - Tensile stress - parallel to grain. DIN Handbook. German Institute for Standardization

Deomano, E.C., Zink-Sharp, A. (2004). Bending properties of wood flakes of three southern species. Wood and Fiber Science. 36(4): 493-499.

Geimer, R. L., Montrey, H. M., & Lehmann, W. F. (1975). Effects Of Layer Characteristics On The Properties Of Three-Layer Particleboards. Aust. J. Appl. Sci., (3), 125-143.

Geimer, R. L. (1979). Data Basic To The Engineering Design Of Reconstituted Strandboard. In *Proceedings Of The 13t H Washington State University International Symposium On Particleboard* (Pp. 105–125).

Geimer, R.L., Mahoney, R.J., Loehnertz, S.P., Meyer, R.W. (1985). Influence of processing-induced damage on strength of flakes and flakeboards. USDA FPL Research Paper FPL 463.

Haynes, R. W. (2003). *An analysis of the timber situation in the United States: 1952 to 2050*. US Dept. of Agriculture, Forest Service, Pacific Northwest Research Station.

Hilbrand, H. C. (1967). Graphical Solution for Shear Deflection of Flexural Members. Forest Products Journal, 17(6), 61–62.

Hindman, D.P., Lee, J.N. (2007). Modeling wood strands as multi-layer composites: bending and tension loads.. Wood and Fiber Science. 39(4): 515-526.

Hunt, M.O., Triche, M.H., McCabe, G.P., Hoover, W.L. (1989). Tensile properties of yellow-poplar veneer strands. Forest Products Journal. 39(9):31-33.

ISO 3345. (1975). Wood – Determination of ultimate tensile stress parallel to grain. ISO Standards. International Organization for Standardization.

Jeong, G.Y., Hindman, D.P., Finkenbinder, D., Lee, J.N, Lin, Z. (2008). Effect of loading rate and thickness on the tensile properties of wood strands. Forest Products Journal. 58(10):33-37.

Kloot, N.H. (1952). A micro-testing technique for wood. Aust. Aust. J. Appl. Sci., 3: 125-143.

Kretschmann, D. E. (2008). The influence of juvenile wood content on shear parallel, compression, and tension perpendicular to grain strength and mode I fracture toughness of loblolly pine at various ring orientation. *Forest products journal*, *58*(7-8), 89–96.

Najera, J., & Spelter, H. (2001). *Wood-based panels–supply, trade, and consumption*. UN—ECE/FAO Forest Products Annual Market Review, 2000—2001, Geneva, Switzerland: United Nations Publications, 83—100.

Price, E.W. (1976). Determining tensile properties of sweetgum veneer flakes. Forest Products Journal., 26(10): 50-53.

Rosen, B.W. (1967) . The strength and stiffness of fibrous composites. pages 106-120 in L.J. Broutman and R.H.Kkrock Modern Composite Materials. addison-wesley publ co reading mass 581pgs

Spelter, H., McKeever, D. B., Alderman, M., & (US), F. P. L. (2006). *Status and trends: profile of structural panels in the United States and Canada* (Vol. 636). US Dept. of Agriculture, Forest Service, Forest Products Laboratory.

Timoshenko, S. P. (1953). *History of strength of materials* (Vol. 50). McGraw-Hill.

US FPL. (1999). Wood Handbook: Wood As An Engineering Material. US Forest Products Laboratory.

Wu, Q., Cai, Z., Lee, J.N. (2005). Tensile and dimensional properties of wood strands made from plantation southern pine lumber. Forest Products Journal. 55(2):87-92.

Via, B. K., So, C. L., Shupe, T. F., Groom, L. H., & Wikaira, J. (2009). Mechanical response of longleaf pine to variation in microfibril angle, chemistry associated wavelengths, density, and radial position. *Composites Part A: Applied Science and Manufacturing*, *40*(1), 60-66.

Chapter 4

Nondestructive Evaluation Of Wood Strand Mechanical Properties Using Near-Infrared Spectroscopy

Abstract

Near-infrared spectroscopy (NIRS), when coupled with various statistical modeling techniques, has yielded promising results for nondestructive evaluation of wood properties. Previous research has demonstrated the ability to use NIRS to predict wood density, moisture content, modulus of elasticity (MOE), and modulus of rupture (MOR). However, most of the current and published research has focused on NIRS predicting mechanical properties of clear specimens (25 x 25mm or more in cross-section) in flexural tests. The goal of this research is to investigate the ability of NIRS to predict and sort wood strands based on mechanical properties. Strands are utilized in construction of both wood composite panels (OSB) and lumber (OSL). Current production techniques for strand-based composites treat all strands as homogenous in terms of mechanical properties. Monitoring variation in wood strand quality using NIRS prediction models could improve quality control in manufacturing.

In this project, Southern yellow pine (*Pinus spp*) strands were scanned to produce spectra for the near-infrared range from 1000 to 2500nm. Following acquisition of NIR spectra, strands were subjected to bending or tensile stress. Results from mechanical testing were used with sample spectra to produce multiple linear regression (MLR) or principal component regression (PCR) prediction equations for modulus of elasticity (MOE), and modulus of rupture (MOR) or ultimate tensile strength (UTS).

4.1 Introduction

4.1.1 NIRS and Wood Properties Prediction

The goal of engineered wood composites is to design biomaterials that achieve more uniformity in performance attributes such as strength and dimensional stability. Furthermore, wood strand composites seek to utilize strands from smaller diameter trees that cannot be utilized for lumber or veneer.

Near infrared spectroscopy (NIRS) is a known method for rapid nondestructive analysis of both physical and mechanical properties of wood. Table 4.1 is a brief summary of research on using NIRS to predict mechanical properties of solid wood.

Table 4.1 Summary NIRS and Solid Wood Mechanical Properties Literature

Properties	MOE R^2	MOR R^2	Model type	Stress	Reference
MOR		0.29	PLS	Bending	Hoffmeyer 1995
MOE, MOR	0.82-0.87	0.84-0.88	PLS	Bending	Schimleck 2005
MOE	0.55-0.74		PLS	Bending	Thumm & Meder 2001
MOE	0.89		PLS	Bending	Gindl 2001
MOE, MOR	0.71-0.79	0.81-0.88	PLS	Bending	Kelley 2004
MOE, MOR	0.89	0.84	PLS	Bending	Fujimoto 2008
MOE, MOR	0.84-0.89	0.86-0.89	MLR, PCR	Bending	Via 2003
MOE, UTS	0.53-0.74	UTS R^2 0.44-0.74	PLS	Tension	Tsuchikawa 2005

In 1995 Hoffmeyer and Pedersen used NIRS to predict a variety of wood properties including compression and bending strength and stiffness. Tests were conducted on lumber with

a range of characteristics including drying and growth defects. Although prediction of bending properties was not as efficient as physical properties, it was still as effective as visual grading methods (Hoffmeyer & Pedersen 1995). Thumm and Meder (2001) utilized NIRS to predict strength and MOE in bending for radiata pine (*Pinus radiata).* In addition to scanning static clear samples, samples were also scanned moving at a rate of 900mm/min. Prediction models were built using raw, 1st, and 2nd derivative of the spectra. The best results (R^2=0.74) were achieved using the 1st derivative of NIR spectra with outliers removed (Thumm & Meder 2001). Gindl et al. (2004) performed similar tests on clear samples of European larch. They found mechanical properties of samples with compression wood could be predicted with NIR spectra, supporting the fact that NIRS is sensitive to more than just wood density and other factors (such as microfibril angle) are indirectly measured due to associated chemical composition of wood (Gindl et al. 2001). Kelley et al. (2004) used NIRS to investigate the physical and mechanical properties of loblolly pine (*Pinus taeda*). Samples were analyzed using both full-range (500-2500nm) and limited-range (650-1150nm) spectra. Results from full and reduced range were similar with a maximum R^2 0.88 for MOE (Kelley et al. 2004). Via et al. (2003) used NIRS to model strength and stiffness of longleaf pine (*Pinus palustris*) using clear samples and both multiple linear regression (MLR) and principal component regression (PCR). They observed that NIRS models built from mature wood spectra were not suitable for predicting mechanical properties of juvenile wood (Via et al. 2003). In 2005, Via et al. investigated the ability to use NIRS for southern yellow pine species in the presence of blue stain. It was found that models could be built that were insensitive to blue stain sensitive wavelengths, but differences in NIR spectrometers can introduce bias (Via et al. 2005). In addition to the summary in Table 4.1, a significant amount of research involving flexural properties and NIRS has been published (Via et

al. 2005, Jones et al. 2005, Andre et al. 2006, Lestander et al. 2008, Via et al. 2009, Horvath et al. 2010). However, very little research involving predictions of tensile properties of wood using NIRS has been published. Tsuchikawa et al. (2005) investigated NIRS and tensile properties in 2005 using Japanese species. Tensile tests were conducted according to Japanese Industrial Standards, and yielded an R^2 of 0.53-0.74 for tensile MOE and 0.44-0.74 for ultimate tensile strength (UTS) (Tsuchikawa et al. 2005).

NIRS has also been shown to be useful in a manufacturing environment. Thumm et al. first investigated scanning of moving samples in 2001 (Thumm et al. 2001). Based on the findings a trial was conducted at a full-scale sawmill. The trial showed promise but was conducted on green cants, not lumber or strands (Meder et al. 2003). Fujimto et al. investigated the feasibility of on-line grading of sawn lumber using NIRS with Japanese larch (*Larix kaempferi*). Samples were scanned while moving past the spectrometer at a rate of 10m/min. Predictions were compared to static bending results and the R^2 ranged from 0.50-0.71 for MOE and 0.19-0.53 for MOR. The ratio of performance to deviation (RPD) ranged from 1.55-2.26 for MOE and 1.66-13.54 for MOR (Fujimoto et al. 2010). NIRS was utilized as a tool for improving production of laminated veneer lumber (LVL) panels in 2002. Meder et al. (2002) scanned individual veneers using NIRS and then correlated spectra against stiffness data obtained from LVL panels assembled from the same population of veneers. The method showed promise with MOE predicted with an R^2 of 0.59 for raw spectra, and 0.74 for 1st derivative spectra (Meder et al. 2002).

4.1.2 NIRS and Wood Property Interpretation

Wood is a composite material at the macro-, micro-, and molecular level. Although sensitive to macro- characteristics (such as density), NIRS is primarily a tool for analysis of

chemical composition at the molecular level. The strength of wood is derived from its three constituent polymers: cellulose, hemicellulose, and lignin (Kollmann & Coté 1968). Cellulose is oriented linearly and is composed of both crystalline and amorphous regions. Since cellulose lacks affinity for lignin, it is encased by hemicellulose. The hemicellulose is in turn encrusted by phenolic lignin. All three polymers exhibit vastly different mechanical properties, and each plays a major role in wood strength.

Below the proportional limit, it is believed that intermolecular bonds between cellulose chains are responsible for strength of the molecule. Once shear forces develop between adjacent cellulose chains, C3-C5 hydrogen bonds begin to break. The chains then slide and hydrogen bonds are reformed without permanent deformation of wood material as stresses are contained and distributed within individual wood cells, though within rings C-C and C-O bonds may be temporarily distorted. Figure 4.1 is a graphical representation of the aforementioned phenomena with A representing initial arrangement of cellulose chains, B shows the breaking of bonds between adjacent cellulose chains, and C shows new bonds forming between adjacent chains. Thus cellulose is extremely resistant to tensile stresses due to covalent bonding between units and within a pyranose ring, while allowing for elastic deformation at hydrogen bonds (Winandy & Rowell 1984).

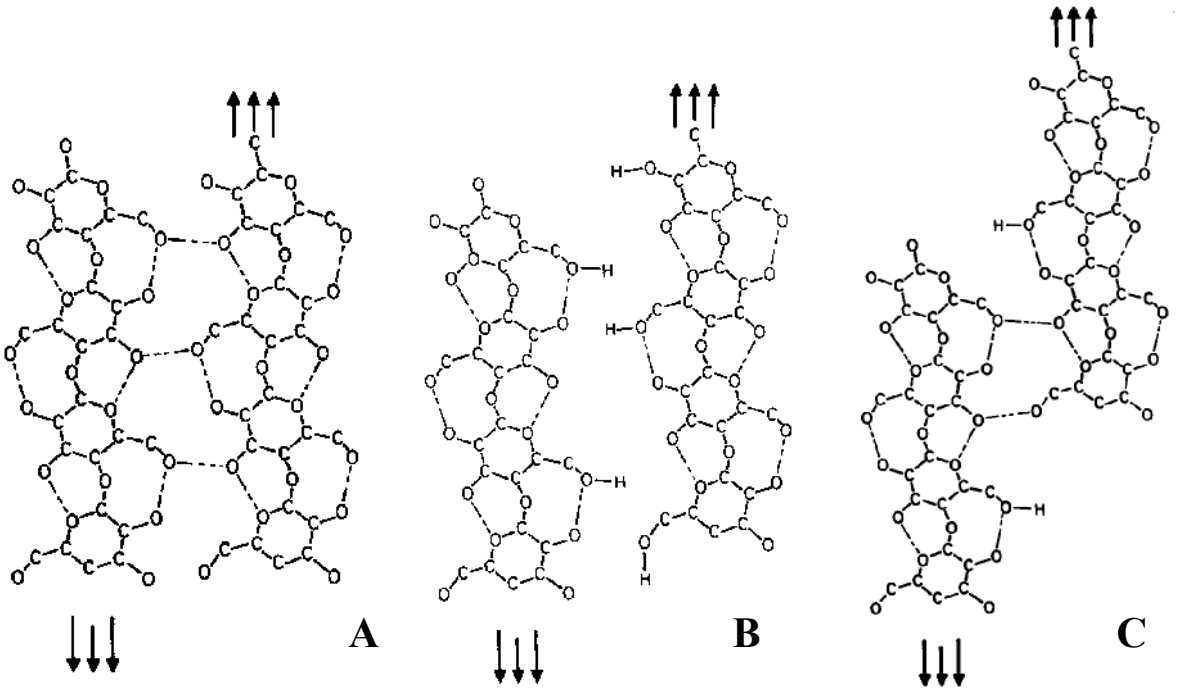

Figure 4.1 Theoretical deformation of cellulose chains (Winandy & Rowell 1984)

Beyond the proportional limit hemicellulose and lignin become much more important in wood strength (Gindl et al. 2004). It is hypothesized, in the Velcro mechanics approach to wood deformation, that wood undergoes a stick-slip mechanism similar to that exhibited by ductile metals. Once the shear stress in the cellulose-hemicellulose matrix exceeds the bonds strength, the bonds break, and additional deflection occurs. When the stress is released, new bonds form between the cellulose chain and the hemicellulose matrix, the chains do not return to the original position. In essence the hemicellulose side chains act as Velcro hooks to the cellulose chains (Kretschmann 2003).

Furthermore, during plastic deformation, stresses begin to rupture the C-C and C-O covalent bonds within polymers. It is believed C-C bonds begin failing in three specific regions: at and through lignin-hemicellulose interface parallel to cellulose chains, depolymerization of hemicellulose, and depolymerization amorphous cellulose. Eventually failure will occur within

crystalline cellulose, resulting in disintegration of wood at molecular level (Robinson 1921, Jeronimidis 1980, Winandy & Rowell 1984, Lucas et al. 1995).

It is often assumed that the crystalline and semi-crystalline regions of cellulose impact the elastic stiffness of wood, whereas the mechanical properties reflecting both the elastic and plastic deformation of wood (MOR, UTS) will be influenced by all constituent polymers. Since NIRS is sensitive to the various polymers and bonds within wood, it becomes a powerful tool for interpretation of chemistry and wood strength. Table 4.2 is a summary of the wavelengths associated with the various polymers and chemical bonds observed during interpretation of NIRS spectra.

Table 4.2 Assignment of absorption bands to important wood chemistry constituents

	Wavelength (nm)	Polymer/chemistry assignment	Reference
1	1130-1135	Aromatic portion of lignin	Tsuchikawa et al. 2004, Terdongworakul et al. 2005, Via et al. 2009
2	1423-1428	Amorphous region of cellulose	Tsuchikawa & Siesler 2003, Tsuchikawa et al. 2004, Via et al. 2009
3	1476	Semi-crystalline regions of cellulose	Tsuchikawa & Siesler 2003
4	1548-1592	C3-C5 intramolecular bond, Crystalline regions of cellulose	Tsuchikawa & Siesler 2003, Tscuchikawa et al. 2004, Via et al. 2009
5	1672	Aromatic portion of lignin	Siesler et al. 2002, Soukupova et al 2002, Tsuchikawa et al. 2004, Yeh et al. 2004, Terdongworakul et al. 2005, Via et al. 2009
6	1724	Furanose/pyranose due to hemicellulose	Osborne et al. 1986, Tsuchikawa et al. 2005
7	1758	Alpha cellulose	Terdongworakul et al. 2005, Via et al. 2009
8	1790-1830	Semi-crystalline or crystalline regions of cellulose	Osborne et al. 1986, Tsuchikawa et al. 2005
9	2080	Semi-crystalline or crystalline regions of cellulose	Osborne et al. 1986, Tsuchikawa et al. 2005
10	2140	Amorphous regions of cellulose	Osborne et al. 1986, Tsuchikawa et al. 2005
11	2200	CHO	Osborne et al. 1986, Tsuchikawa et al. 2005
12	2336	Semi-crystalline or crystalline regions of cellulose	Osborne et al. 1986, Tsuchikawa et al. 2005

In their interpretation of NIRS prediction models, Tsuchikawa et al. (2005) identified polymers and chemical groups and the associated wavelengths that effect mechanical properties. Tsuchikawa et al. (2005) analyzed two different wood species, a hardwood (Japanese zelkova: *Zelkova serrata*) and Japanese red pine (*Pinus densiflora*). In the pine species, cellulose associated wavelengths were key factors for MOE prediction. Furthermore, increases in the crystalline cellulose and decreases in amorphous cellulose resulted in increased MOE. The same relationships were found for UTS. Such relations were not observed for Japanese zelkova, instead all principal constituents were factors for prediction of MOE and UTS (Tsuchikawa et al. 2005).

Via et al. (2009) conducted similar analysis of NIRS and wavelengths associated with mechanical properties. Via et al. (2009) identified wavelengths associated with crystalline cellulose to be important for MOE prediction. Decreases in wavelengths associated with lignin resulted in lower observed MOR. Furthermore, alpha cellulose associated wavelengths and hemicellulose associated wavelengths were important for prediction of both MOE and MOR. When analyzing juvenile wood and mature wood separately Via et al. (2009) observed lignin associated wavelengths to be more important for MOE and MOR in juvenile wood, while cellulose associated wavelengths were more important for MOE and MOR in mature wood (Via et al. 2009).

Based on the reviewed literature it is known that NIRS is a powerful tool for nondestructive evaluation of solid wood and veneers in both flexural and tensile stresses. It is the goal of this research to test NIRS as a nondestructive tool for evaluating mechanical properties of wood strands for use in strand-based composites.

4.2 Materials and Methods

4.2.1 Strand Preparation

All wood strands utilized were identified as southern yellow pine (*Pinus spp*.). Plant strands were obtained from LP Hanceville (Hanceville, AL) OSB plant. Flakes were collected from the manufacturing line just before the screening zone. Sawn strands were produced from cutoffs donated by Capitol Truss (Wetumpka, AL) and Dudley Lumber Co (Salem, AL), and boards purchased locally. Different sources of wood were needed to ensure a wide range in mechanical and physical properties. Boards and cutoffs were cut into clear samples 25mm by 25mm by 200mm in length and placed in humidity chamber until processing began.

Plant strands to be used in experimentation were sorted from approximately 1.3 cubic meters of unscreened strands. Radially-cut strands with dimensions of at least 125mm in length and 25mm in width were selected. Strands with splitting or warp (bends, twists, cupping) were not selected. The selected strands were then cut to uniform size using a guillotine paper cutter. To produce sawn strands, the collected lumber cutoffs were first cut into small clear samples measuring 200 x 25 x 25mm. These small clear samples were then ripped along the radial face to produce strands of approximately 200 x 25 x 1.0mm. Both plant and sawn strands were conditioned at 22°C and 50% relative humidity. A total of 150 plant strands were tested: 70 tension samples and 80 flexural samples. A total of 100 sawn strands were tested: 50 in tension, 50 in bending.

4.2.2 Near Infrared Spectroscopy

A Perkin Elmer Spectrum 400 FT-IR/FT-NIR Spectrometer was used to collect the NIR spectra. Absorbance was recorded from 1000 to 2500nm with resolution of 0.5nm. Spectra were

produced for four locations on each strand, with each spectra composed of eight individual scans with a beam diameter of approximately 7mm. Spectra were created from scans at the center and third points of each sample. The four individual spectra for each strand were averaged using Spectrum 6.2 software to produce one average spectra for each wood strand. In Figure 4.2 the red circles represent areas where NIR spectra were collected, the red rectangle is the outline of final testing sample geometry.

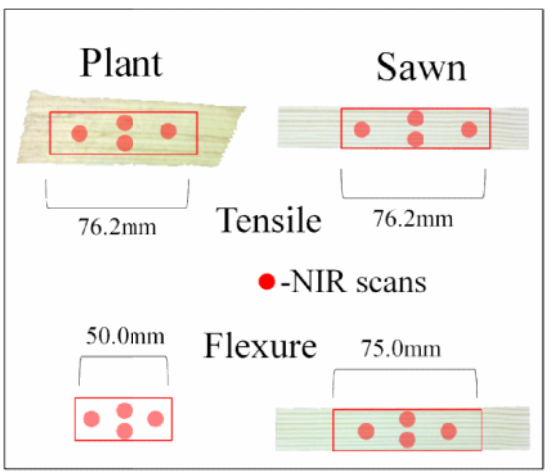

Figure 4.2 NIRS Scan Locations on Strand Samples

Average spectra of all samples are shown in Figure 4.3. The NIR spectra y-axis represents absorption, the x-axis wavelength in nanometer. The NIR spectra baseline can be offset to zero, or pretreated by taking derivative of absorption. By taking the 1st derivative of the spectra, the peaks corresponding to functional groups in wood become more pronounced (as shown in second spectra). This in turn provides a better statistical model as it removes "noise" from the spectra.

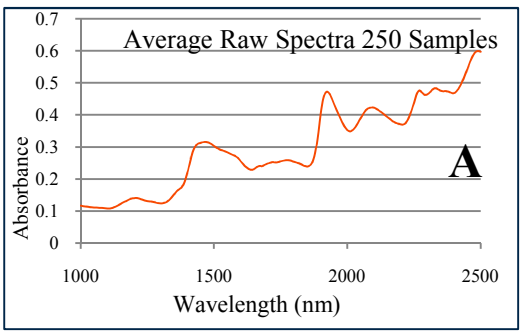

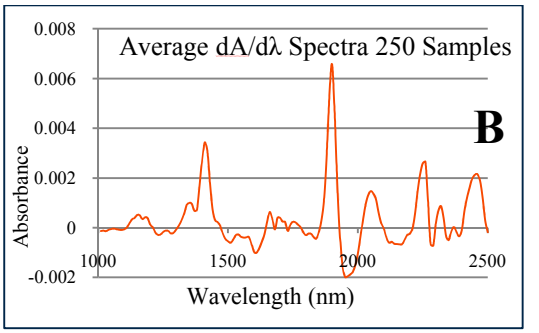

Figure 4.3 Average NIRS Raw (A) and 1st Derivative Spectra (B)

4.2.3 Mechanical Testing

Both axial tension and flexural tests were conducted on the wood strands using a Zwick-Roell load frame equipped with 10kN load cell and a computer controlled screw-drive crosshead. Tensile testing was conducted using screw type grips with a loading rate of 0.254mm/min, a gage length of 50.8mm (Epsilon Corp clip-on extensometer), and grip to grip separation of 76.2mm. Tensile samples exhibiting grip type failures or any failure outside of the gage length were not included in chemometric models. Flexural tests were conducted in three-point setup with loading rate of 4.0mm/min, and support separation of 75mm for sawn strands and 50mm for plant strands (due to end splitting 75mm length was not possible). Testing setups are shown in Figure 4.4.

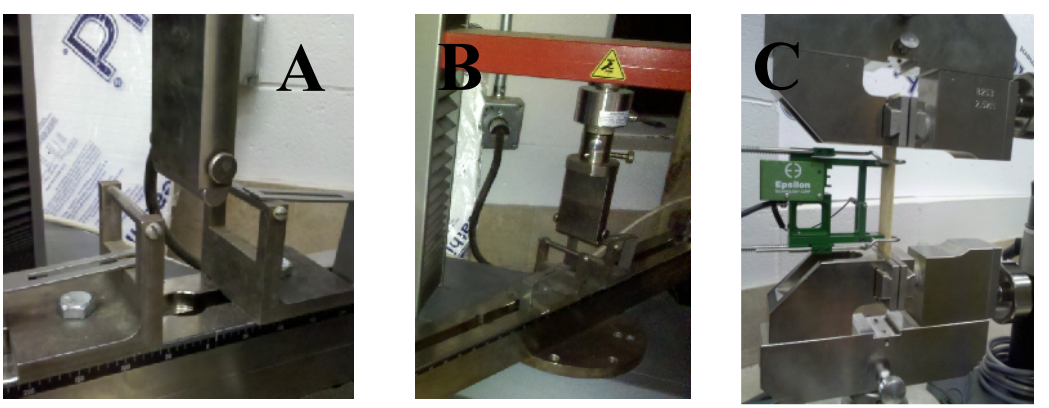

Figure 4.4 Mechanical Testing Setups: Flexural Testing (Close Up) (A), Flexural Testing (With Load Cell) (B), Tensile Testing (C)

4.2.4 Chemometric Technique

Following mechanical testing multiple linear regression (MLR) and principal components regression (PCR) models were created using Quant+ software package. The Quant+ software allowed for spectra pretreatment by taking the 1st derivative of absorption in addition to raw spectra. Models were developed for tensile modulus (ETENS), ultimate tensile strength (UTS), flexural modulus of elasticity (MOE), and ultimate bending strength (MOR). Calibrations were estimated using full-cross validation. Mechanical testing results and spectra were also exported to Microsoft Excel for averaging and interpretation.

Principal components regression (PCR) and Multiple Linear Regression (MLR) models were produced using Perkin Elmer Spectrum Quant+ software package. Separate models were developed for raw and pretreated spectra. Spectra were pretreated to transform original data to 1st derivative or 2nd of absorbance (see Figure 4.3).

4.3 Results & Discussion

4.3.1 Statistical Model Summary

Results of the chemometric models built using absorbance spectra and mechanical results are shown below. A baseline correction of NONE represents the raw spectra, while $dA/d\lambda$ and $d^2A/d\lambda^2$ represent first and second derivative pretreated spectra. PC is the number of principle components or factors used in model (each factor generally corresponds to one or more spectral peaks). The coefficient of calibration (R^2) represents the proportion of property variability accounted for in the model. The ratio of performance to deviation (RPD) is a general indicator of model predictive adequacy (Bailleres et al. 2002). RPD is calculated as standard deviation divided by standard error of prediction (SEP).

Equation 4.1 Calculation of Ratio of Performance to Deviation (RPD)

$$RPD = \frac{standard\ deviation}{SEP}$$

Results for statistical models for the tensile tests are displayed in Table 4.3 and flexural model results are shown in Table 4.4.

Table 4.3 Summary of Calibration Models for Tensile Testing of Strands

Type	Property	Baseline Correction	Model Type	Factors	R^2	SEE	SEP	RPD
Plant	MOE	NONE	MLR	9	0.26	2.78	3.36	0.862
	UTS	NONE	MLR	9	0.37	13.97	16.78	0.957
Plant	MOE	$d^2A/d\lambda^2$	MLR	7	0.12	2.93	3.46	0.823
	UTS	$d^2A/d\lambda^2$	MLR	7	0.30	14.33	16.59	0.931
Sawn	MOE	NONE	MLR	5	0.61	2.05	2.56	1.069
	UTS	NONE	MLR	5	0.37	17.98	21.33	0.889
Sawn	MOE	$d^2A/d\lambda^2$	MLR	4	0.55	2.19	2.47	1.218
	UTS	$d^2A/d\lambda^2$	MLR	4	0.46	10.59	10.99	1.167

Table 4.4 Summary of Calibration Models for Flexural Testing of Strands

Flexural	Property	Baseline Correction	Model Type	PC	R^2	SEE	SEP	RPD
Plant	MOE	NONE	PCR	8	0.48	0.894	1.065	1.07
	MOR	***NONE***	***PCR***	***5***	***0.43***	***12.8***	***15.3***	***1.05***
Plant	***MOE***	***dA/dλ***	***PCR***	***6***	***0.50***	***0.846***	***0.939***	***0.84***
	MOR	dA/dλ	PCR	3	0.35	13.6	16.0	1.02
Sawn	MOE	NONE	PCR	5	0.75	0.624	0.777	1.54
	MOR	NONE	PCR	2	0.45	12.3	13.3	1.22
Sawn	***MOE***	***dA/dλ***	***PCR***	***6***	***0.76***	***0.621***	***0.805***	***1.48***
	MOR	***dA/dλ***	***PCR***	***3***	***0.51***	***11.7***	***13.9***	***1.16***

Italics represent best results and models that will be used for future NDE of wood strand strength and stiffness

As was expected from the literature review, the NIR method was able to evaluate wood strand strength and stiffness in a nondestructive manner. However, the models vary greatly in quality based on R^2, number of prediction factors, and RPD.

4.3.2 Prediction

4.3.2.1 Tensile Model Results

The strongest models for plant strand MOE and UTS were achieved using raw spectra, producing coefficients of determination of 0.26 for MOE and 0.37 for UTS. Likewise the highest RPD for MOE and UTS were achieved using raw spectra (Table 4.3). Actual versus predicted plots are shown in Figure 4.5. Tensile models for sawn strands showed considerably closer agreement with actual data than those for plant strands. The best MOE predictive model was built using the raw spectra which yielded a coefficient of determination of 0.61. For UTS the 2nd derivative spectra yielded better results than the raw spectra, with an R^2 of 0.46. For both MOE and UTS the highest RPD values were reached using 2nd derivative spectra. The models compare well with existing NIRS and tensile testing research that has produced R^2 ranging from 0.53 to 0.74 for MOE using samples from one board (Tsuchikawa et al. 2005). The best models for MOE were produced using the 2nd derivative spectra which removes baseline shift associated with density. Since the models were linear in nature, removing density as a factor would better predict tensile stiffness as the relationship between tensile stiffness and density is nonlinear (Biblis 1968, Geimer et al. 1985).

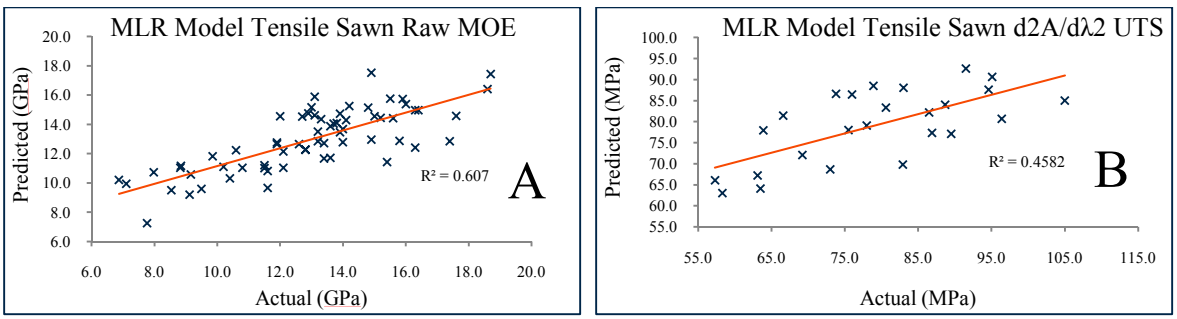

Figure 4.5 Tensile Model Actual Values versus Predicted Values for MOE (A) and UTS (B)

It is also important to note this research utilized samples from different trees, rather than samples cut from one board. It is known that mechanical properties and associated chemical properties increase when moving away from pith to bark and along the bole (Via et al. 2009). Therefore it is expected that the R^2 in NIRS models built from one tree or board will be higher than those taking into account variation between trees. Sawn strand models were expected to provide better results compared to plant strand models as a result of manufacturing defects (Geimer et al. 1985). NIRS can only account for chemical and density differences between samples; manufacturing defects (such as internal voids and cracks) may not affect NIRS spectra, but would greatly reduce the strength. The sawn samples, being prepared in a controlled setting with a bandsaw, did not have the same defects created during stranding.

4.3.2.2 Flexural Model Results

Models produced from the spectra and flexural properties were significantly better than tensile models. This is a result of consistent and predictable failure location achieved through flexural testing. Furthermore, flexural testing takes into account the entire cross section of sample, whereas tensile testing results are more dependent on the weakest portion of the specimen (especially true in non-uniform materials such as wood). That is to say a single point of weakness, such as a severed tracheid or local area of low density, will greatly reduce the

ability of a sample to carry proportional loads leading to premature failure (Biblis 1970, Geimer et al. 1985). Plots for actual versus predicted flexural MOE and MOR are shown in Figure 4.6.

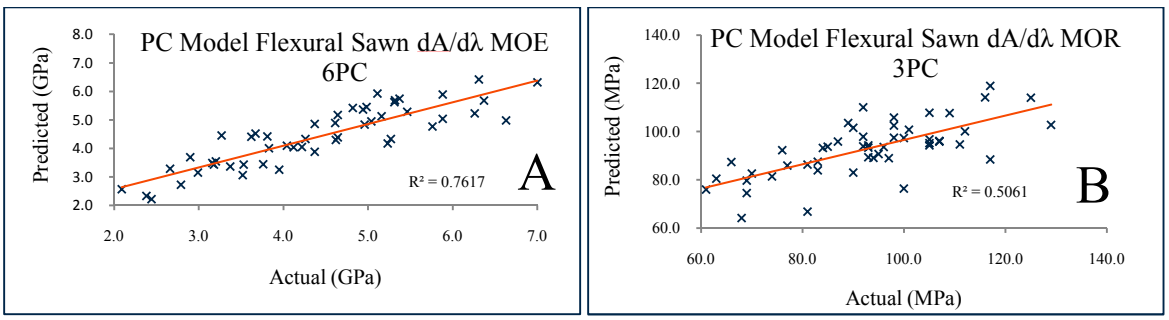

Figure 4.6 Flexural Model Actual Values versus Predicted Values for MOE (A) and MOR (B)

As with tensile models, flexural models performed better for sawn strands than plant strands. This is most likely the result of manufacturing defects present in plant strands that are not present in sawn strands. The strongest model for MOE of plant strands was created using the 1st derivative of the spectra with an R^2 of 0.50. The strongest MOR model for plant strands was created using raw spectra with R^2 of 0.43. The best calculated RPD for plant models were 0.84 for MOE and 1.05 for MOR. With sawn strand samples models for MOE and MOR were strongest using 1st derivative spectra, with R^2 of 0.76 for MOE and an R^2 of 0.51 for MOR. RPD values for MOE and MOR were 1.48 and 1.16 respectively (Table 4.4).

4.3.3 Interpretation

For interpretation of key spectroscopic features used in prediction of mechanical properties, regression of PC's (as independent variables) were produced from MLR and PCR analysis to predict the strength and stiffness of strands in tension and bending. Key wavelengths are labeled according to Table 4.2. Wavelengths for associated groups found in Table 4.2 are a

rough guide, as using different spectrometer often results in slight shifts in spectral peaks (Via et al. 2006).

In the regression spectrum for tensile MOE of sawn strands, key wavelengths associated with cellulose were most dominant (Figure 4.7). Wavelengths for the crystalline regions of cellulose (4) and semi-crystalline or crystalline regions of cellulose (8, 9, 10, 12) were most dominant. This observation supports both the chemistry model of strength proposed by Winandy & Rowell (1984). Furthermore, the strong presence of lignin (5) and amorphous cellulose regions (3), are in agreement with the findings of Tsuchikawa et al. (2005).

The similarities between regression spectra for MOE and UTS of strands in tension further supported the proposed chemistry model of strength (Winandy & Rowell 1984). In tension, the microfibrils are stressed in axial tension along their length. As stated earlier, it is believed the C3-C5 and intramolecular hydrogen bonds would be the most important. However, in juvenile wood, due to high microfibril angle, microfibrils are not loaded in parallel. In this case, the lignin plays a higher role in transfer of stresses, specifically above the elastic limit. For these reasons aromatic portions of lignin (5) appear in both MOE and MOR regression spectra. It's important to note the aromatic portion of lignin (5) is more pronounced in MOR, which includes the plastic response of wood in tension, than in MOE, which only accounts for elastic response. Via et al. (2009) found similar results while investigating regression spectrum of both juvenile and mature wood.

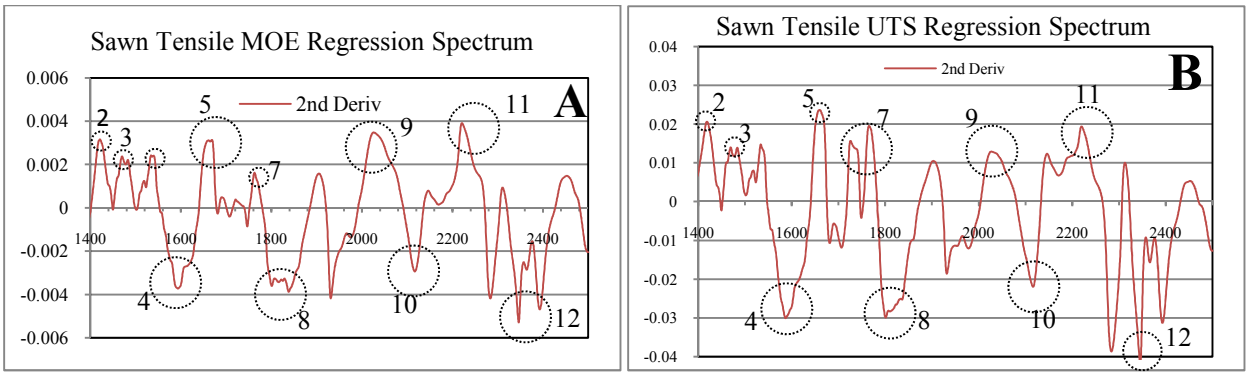

Figure 4.7 Regression Spectrum for Tensile Models for MOE (A) and UTS (B)

As with tensile associated spectra, key wavelengths and associated groups in flexural model regression spectrum (Figure 4.8) are labeled according to Table 4.2. Again, the wavelengths for associated groups found in Table 4.2 are a rough guide, as using different spectrometer often results in slight shifts in spectral peaks (Via et al. 2006).

In the flexural MOE regression spectrum, wavelengths for cellulose (2, 4, 7, 9, 10, 12), hemicellulose (6), and lignin (1, 5) are present. The most dominant wavelengths in the MOE regression spectrum are those attributed to crystalline cellulose (4) and semi-crystalline or crystalline regions of cellulose (12). This supports the Winandy & Rowell (1984) theory of chemistry and wood strength, in which cellulose is the dominant polymer in wood strength below the elastic limit. The presence of alpha cellulose related wavelength (7) concurs with the findings of Via et al. (2009) who found alpha cellulose to be an important factor for prediction of MOE and MOR. Also, the regression spectra for flexural MOE was built using PCR, and hemicellulose associated wavelengths (6) were important factors. This is in agreement with the findings of Via et al. (2009) who found hemicellulose to be an important factor for MOE when using PCR models, but not when using MLR models due to multicollinearity with other wavelengths.

Beyond the elastic limit in flexure, unlike in tension, hemicellulose and lignin polymers are expected to resist stresses as they are transferred from cellulose microfibrils to the surrounding hemicellulose-lignin matrix. As a result, cellulose related wavelengths (2, 3, 4, 8, 10, 12) remain important, but lignin related wavelengths (1) become more important than under purely elastic circumstances. Alpha cellulose related wavelengths (7) were not important, and this is attributable to the presence of juvenile wood samples in the prediction model (Via et al. 2009). Furthermore, hemicellulose related wavelengths (6) were not particularly important for MOR models, which agrees with findings of Via et al. (2009). The high importance of the aromatic portion of lignin (1) also agrees with findings of Via et al. (2009) who proposed that higher microfibril angles in juvenile wood resulted in increased loading of lignin. Gindl et al. (2004) and Winandy & Rowell (1984) have previously stated the importance of lignin in wood strength beyond the elastic limit. It is interesting to note that alpha cellulose related wavelengths (2) are more pronounced in the MOR regression spectrum than in the MOE regression spectrum. Although it is known that the crystalline regions are stiffer than the amorphous regions, the plastic response of amorphous cellulose is not fully understood (Keckes et al. 2003). However, the presence of amorphous cellulose related wavelengths in MOR regression spectra indicates the amorphous region plays an important role in the plastic response of wood.

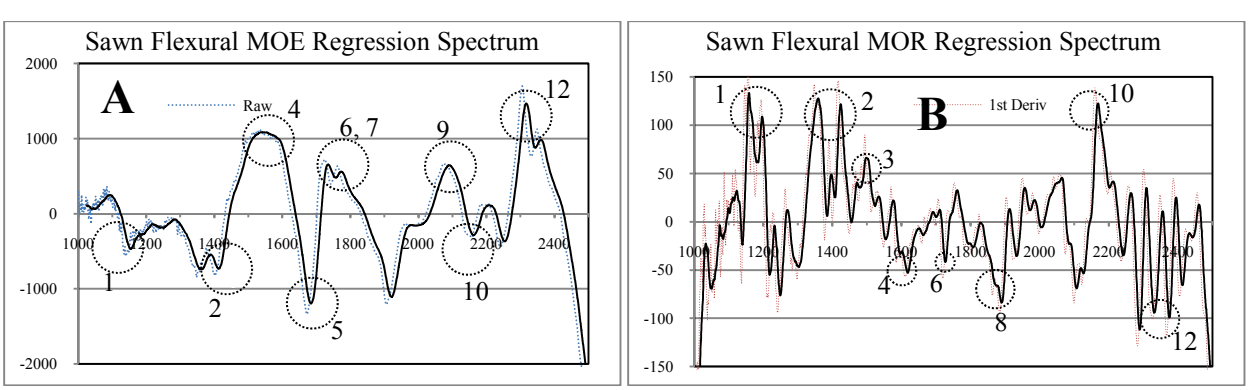

Figure 4.8 Regression Spectrum for Flexural Models MOE (A) and MOR (B)

4.4 Practical Implications

Since the ultimate goal of this research is to develop a method of producing strand-based composites using NIRS, it is important to look at practical implications. NIRS has already been effectively used at production speeds to analyze sawn-lumber mechanical properties (Fujimoto et al. 2010). It is known that the quality of wood composites is highly correlated with the quality of strands used in production (Deomano & Zink-Sharp 2004). Therefore juvenile wood poses a unique problem for composite panel manufacturers as it is known to be inferior to mature wood in mechanical properties (US FPL 1999). Adding to the problem is the silvicultural methods that lead to a higher prevalence of juvenile wood in American timber (Zobel 1984). However, the NIRS method of nondestructive evaluation of mechanical properties would help the manufacturer to monitor the presence of juvenile wood entering the production process. While the R^2 and RPD of the best models (Table 4.4) for MOE (R^2 0.76, RPD 1.48) and MOR (R^2 0.51, RPD 1.16) were not strong enough for prediction of single strand properties, they were sufficient for general rough screening which requires R^2 between 0.50 and 0.64 (Williams 2004). It is also important to note that production of panels only requires panels to exceed some lower limit. Meaning the overall mean strength of panels is not as important as controlling variation to ensure all panels are above some lower limit. As a result NIRS systems have led to cost savings in trial runs at a particleboard plant (Sjöblom et al. 2004). Also, the calibration model strength may have been impacted by manufacturing or other defects that reduce apparent strength in testing. When used in composites such defects are often reduced through lignin flow. Plasticization of wood causes lignin to mend internal fractures that may be incurred during manufacturing (Spalt 1976, Geimer et al. 1985). In use, the NIRS system could be used to monitor wood quality by detecting changes in wood spectra. Changes in wood spectra could indicate presence of juvenile

wood or other undesirable traits in wood furnish. This data could then be used to alter production process downstream, such as mat height, resin content, and pressing parameters. This method for monitoring strand quality in a production environment becomes more attractive when one considers the changes in production and resin formulations.

Formaldehyde based resins are the most commonly used in production of wood composites such as oriented strandboard. Although formaldehyde has been safely used in wood composites, the possible negative health and environmental effects of formaldehyde resin in wood composites have been researched for quite some time (Nestler 1977, Meyer & Hermanns 1985). In response, the wood composites industry has developed resins based on low-formaldehyde and formaldehyde-free resins. While better from a health and environmental standpoint, these new resins are far more sensitive to production variations, including variation in wood raw material (Gylseth & Maylor 1996). While initial attempts at reducing formaldehyde resin in wood were proactive, changes in law are forcing producers to comply with stricter standards. In 2009 the California Air Resources Board (CARB) imposed title 17: "Airborne Toxic Control Measure to Reduce Formaldehyde Emissions From Composite Wood Products," which limits formaldehyde emissions from wood composites shipped and sold in California (CARB 2007). In 2010 a bill, S.1660 - Formaldehyde Standards for Composite Wood Products Act, was amended to the Toxic Substance Control Act to reduce formaldehyde content and emission in wood products nationwide (111th US Congress Senate Bill 1660 2010). These new restrictions on formaldehyde will undoubtedly require wood composite manufacturers to better control variation throughout production. On-line NIRS monitoring of wood strand quality could be effective method to control variation in composite manufacturing.

4.5 References

Andre, N., Labbe, N., Rials, T., & Kelley, S. (2006). Assessment Of Wood Load Condition By Near Infrared (NIR) Spectroscopy. *Journal Of Materials Science*, *41*(7), 1879-1886. Doi: 10.1007/S10853-006-4433-6.

ASTM. (2000). Annual book of ASTM Standards. Section, 4.

Baillères, H., Davrieux, F., & Ham-Pichavant, F. (2002). Near infrared analysis as a tool for rapid screening of some major wood characteristics in a eucalyptus breeding program. *Annals of forest science*, *59*(5-6), 479–490.

Biblis, E.J. (1968). Transitional variation and relationships among properties within loblolly pine growth ring. Unpublsihed report. Department of Forestry, Auburn University, Auburn, AL.

Biblis, E. J. (1970). Effect of thickness of microtome sections on their tensile properties. *Wood and Fiber Science*, *2*(1), 19–30.

Bodig, J., & Jayne, B. A. (1982). Mechanics Of Wood And Wood Composites. *Van Nostrand Reinhold Co., New York, NY*, *7*, 12.

Californa Air Resources Board (2007). Airborne Toxic Control Measure (ATCM) to Reduce Formaldehyde Emissions from Composite Wood Products. sections 93120-93120.12, title 17, California Code of Regulations (CCR),

Deomano, E., & Zink-Sharp, A. (2004). Bending Properties of Wood Flakes of Three Southern Species. *Wood and Fiber Science*, *36*(4), 493-499.

Fujimoto, T., Kurata, Y., Matsumoto, K., & Tsuchikawa, S. (2008). Application Of Near Infrared Spectroscopy For Estimating Wood Mechanical Properties Of Small Clear And Full Length Lumber Specimens. *JOURNAL OF NEAR INFRARED SPECTROSCOPY*, *16*(6), 529-537. Doi: 10.1255/Jnirs.813.

Fujimoto, T., Kurata, Y., Matsumoto, K., & Tsuchikawa, S. (2010) Feasibility of near-infrared spectroscopy for on-line grading of sawn lumber. *Applied Spectroscopy,* 64(1): 92-99.

Geimer, R.L., Mahoney, R.J., Loehnertz, S.P., Meyer, R.W. (1985). Influence of processing-induced damage on strength of flakes and flakeboards. USDA FPL Research Paper FPL 463.

Gindl, W., Gupta, H. S., Sch\öberl, T., Lichtenegger, H. C., & Fratzl, P. (2004). Mechanical properties of spruce wood cell walls by nanoindentation. *Applied Physics A: Materials Science & Processing*, *79*(8), 2069–2073.

Gylseth, B., & Maylor, R. (1996). New melamine modified binders for low formaldehyde emission wood panels. *Asian Timber, September*, 52–55.

Hoffmeyer, P., & Pedersen, J. G. (1995). Evaluation Of Density And Strength Of Norway Spruce Wood By Near Infrared Reflectance Spectroscopy. *Holz Als Roh-Und Werkstoff*, *53*(1), 165–170.

Horvath, L., Peszlen, I., Peralta, P., & Kelley, S. (2010). Use of transmittance near-infrared spectroscopy to predict the mechanical properties of 1- and 2-year-old transgenic aspen. *Wood Science and Technology,* 45(2),303-314.

Jeronimidis, G. (1980). The fracture behaviour of wood and the relations between toughness and morphology. *Proceedings of the Royal Society of London. Series B, Biological Sciences*, *208*(1173), 447–460.

Jones, P. D., Schimleck, L. R., Peter, G. F., Daniels, R. F., & Clark Iii, A. (2005). Nondestructive Estimation Of Pinus Taeda L. Wood Properties For Samples From A Wide Range Of Sites In Georgia. *Canadian Journal Of Forest Research*, *35*(1), 85–92.

Keckes, J., Burgert, I., Fruhmann, K., Muller, M., Kolln, K., Hamilton, M., Burghammer, M., et al. (2003). Cell-wall recovery after irreversible deformation of wood. *Nat Mater*, *2*(12), 810-813.

Kelley, S. S., Rials, T. G., Snell, R., Groom, L. H., & Sluiter, A. (2004). Use Of Near Infrared Spectroscopy To Measure The Chemical And Mechanical Properties Of Solid Wood. *Wood Science And Technology*, *38*(4), 257–276.

Kollmann, F. F. P., & Coté, W. A. (1968). Principles of wood science and technology. I. Solid wood.

Kretschmann, D. (2003). Natural materials: Velcro mechanics in wood. *Nature Materials*, *2*(12), 775–776.

Lestander, T. A., Lindeberg, J., Eriksson, D., & Bergsten, U. (2008). Prediction Of Pinus Sylvestris Clear-Wood Properties Using NIR Spectroscopy And Biorthogonal Partial Least Squares Regression. *Canadian Journal Of Forest Research*, *38*(7), 2052–2062.

Lucas, P. W., Darvell, B. W., Lee, P. K. D., Yuen, T. D. B., & Choong, M. F. (1995). The toughness of plant cell walls. *Philosophical Transactions of the Royal Society of London. Series B: Biological Sciences*, *348*(1325), 363.

Meder, R., Thumm, A., & Bier, H. (2002). Veneer stiffness predicted by NIR spectroscopy calibrated using mini-LVL test panels. *Holz als Roh- und Werkstoff*, 60:159-164.

Meder, R., Thumm, A., & Marston, D. (2003). Sawmill trial of at-line prediction of recovered lumber stiffness by NIR spectroscopy of *Pinus radiata* cants. *Journal of Near Infrared Spectroscopy,* 11: 137-143.

Meyer, B., & Hermanns, K. (1985). Formaldehyde release from wood products: an overview. *ACS symposium series* (Vol. 16).

Nestler, F. H. (1977). *The Formaldehyde Problem in Wood-Based Products–An Annotated Bibliography.* DTIC Document.

Osborne, B. G., Fearn, T., & Hindle, P. H. (1986). *Near infrared spectroscopy in food analysis*. Longman scientific and technical Essex, England, United Kingdom.

Robinson, W. (1921). The Microscopical Features of Mechanical Strains in Timber and the Bearing of these on the Structure of the Cell-Wall in Plants. *Philosophical Transactions of the Royal Society of London. Series B, Containing Papers of a Biological Character*, *210*, 49–82.

Schimleck, L. R., Jones, P. D., Clark, A. I., Daniels, R. F., & Peter, G. F. (2005). Near Infrared Spectroscopy For The Nondestructive Estimation Of Clear Wood Properties Of Pinus Taeda L. From The Southern United States. *Forest Products Journal*, *55*(12), 21–28.

111th US Congress Senate Bill 1660 (2010) Formaldehyde Standards for Composite Wood Products Act, S. 1660

Siesler, H. W., Ozaki, Y., Kawata, S. and Heise, H. M. (eds) (2002) Near-Infrared Spectroscopy: Principles, Instruments, Applications, Wiley-VCH Verlag GmbH, Weinheim, Germany.

Sjöblom, E., Johnsson, B., & Sundström, H. (2004). Optimization of particleboard production using NIR spectroscopy and multivariate techniques. *Forest products journal*, *54*(6), 71–75.

Soukupova, J., Rock, B. N., & Albrechtova, J. (2002). Spectral characteristics of lignin and soluble phenolics in the near infrared- a comparative study. *International Journal of Remote Sensing*, *23*(15), 3039-3055.

Spalt, H. A. (n.d.). Chemical changes in wood associated with wood fiberboard manufacture. *Wood technology: Chemical aspects. Am. Chem. Soc. Symp. Ser* (Vol. 43, pp. 193–219).

Terdwongworakul, A., Punsuwan, V., Thanapase, W., Tsuchikawa, S. (2005). Rapid assessment of wood chemical properties and pulp yield of Eucalpytus camaldulensis in Thailand tree plantations by near infrared spectroscopy for improving wood selection for high quality pulp. *Journal of Wood Science*, 51(2):167–71.

Thumm, A., & Meder, R. (2001). Stiffness Prediction Of Radiata Pine Clearwood Test Pieces Using Near Infrared Spectroscopy. *Journal Of Near Infrared Spectroscopy*, *9*, 117.

Tsuchikawa, S., & Siesler, H. W. (2003). Near-Infrared Spectroscopic Monitoring of the Diffusion Process of Deuterium-Labeled Molecules in Wood. Part II: Hardwood. *Applied Spectroscopy*, *57*(6), 675-681.

Tsuchikawa, S., Inoue, K., Mitsui, K. (2004) Spectroscopic monitoring of wood characteristics variation by light-irradiation. *Forest Products Journal,.* 54(11), 71–76.

Tsuchikawa, S., Hirashima, Y., Sasaki, Y., & Ando, K. (2005). Near-Infrared Spectroscopic Study Of The Physical And Mechanical Properties Of Wood With Meso-And Micro-Scale Anatomical Observation. *Applied Spectroscopy*, *59*(1), 86–93.

US FPL. (1999). Wood Handbook: Wood As An Engineering Material. US Forest Products Laboratory.

Via, B. K., Shupe, T. F., Groom, L. H., Stine, M., & So, C. L. (2003). Multivariate Modelling Of Density, Strength And Stiffness From Near Infrared Spectra For Mature, Juvenile And Pith Wood Of Longleaf Pine (Pinus Palustris). *Journal Of Near Infrared Spectroscopy*, *11*(5), 365–378.

Via, B. K., So, C., Shupe, T. F., Eckhardt, L. G., Stine, M., & Groom, L. H. (2005). Prediction Of Wood Mechanical And Chemical Properties In The Presence And Absence Of Blue Stain Using Two Near Infrared Instruments. *Journal Of Near Infrared Spectroscopy*, *13*(4), 201.

Via, B. K., Eckhardt, L. G., So, C. L., Shupe, T. F., Groom, L. H., & Stine, M. (2006). The response of visible/near infrared absorbance to wood-staining fungi. *Wood and fiber science*, *38*(4), 717–726.

Via, B. K., So, C. L., Shupe, T. F., Groom, L. H., & Wikaira, J. (2009). Mechanical Response Of Longleaf Pine To Variation In Microfibril Angle, Chemistry Associated Wavelengths, Density, And Radial Position. *Composites Part A*, *40*(1), 60–66.

Williams, P., & PDK Projects, I. (2004). *Near-infrared Technology: Getting the Best Out of Light: a Short Course in the Practical Implementation of Near-infrared Spectroscopy for the User*. PDK Projects, Inc.

Winandy, J. E., & Rowell, R. M. (1984). The chemistry of wood strength. *The Chemistry of solid wood. American Chemical Society, Washington, DC*, 211–256.

Yeh, T.-F., Chang, H.-min, & Kadla, J. F. (2004). Rapid Prediction of Solid Wood Lignin Content Using Transmittance Near-Infrared Spectroscopy. *Journal of Agricultural and Food Chemistry*, *52*(6), 1435-1439.

Zobel, B. (1984). The changing quality of the world wood supply. *Wood Science and Technology*, *18*(1), 1-17.